MARMARA UNIVERSITY
INSTITUTE FOR GRADUATE STUDIES IN PURE AND APPLIED SCIENCES

INVESTIGATION OF HEAVY METAL ION REMOVAL BY CELLULOSE BASED ADSORBENTS WITH IONIC FUNCTIONAL GROUPS

ABDIFATAH ABDI HASHI

MASTER THESIS

Department of Environmental Engineering

Thesis Supervisor

Prof. Dr. Zehra Semra CAN

ISTANBUL, 2023

MARMARA UNIVERSITY
INSTITUTE FOR GRADUATE STUDIES IN PURE AND APPLIED SCIENCES

INVESTIGATION OF HEAVY METAL ION REMOVAL BY CELLULOSE BASED ADSORBENTS WITH IONIC FUNCTIONAL GROUPS

ABDIFATAH ABDI HASHI
524320993

MASTER THESIS
Department of Environmental Engineering

Thesis Supervisor
Prof. Dr. Zehra Semra CAN

ISTANBUL, 2023

ACKNOWLEDGMENTS

The first prize is to Allah, He has given me strength and encouragement throughout all the difficult times of finishing this dissertation. I sincerely appreciate all His mercy, grace, and unending love.

I want to take this opportunity to show sincere appreciation to my supervisor, Prof. Dr. Zehra Semra Can, for the constant supervision and insightful feedback. I am very grateful to Marmara University, Institute of Pure and Applied Sciences for giving me the opportunity to acheive master's study.

I want to take this opportunity to show sincere appreciation to the members of my master's thesis committee, Assoc. Prof. Dr. Esra Erken, and Assist. Prof. Dr. Muhammet Ceylan, for their critical reviews of my work, and their valuable contributions.

I gratefully acknowledge Prof. Dr. Othman Hamed from An-Najah National University and Assoc. Prof. Dr. Abdalhadi Deghles from Al-Istiqlal University for the production of foam materials. I also would like to thank the Middle East Technical University Central Laboratory for conducting FTIR, BET, and SEM tests for the characterization of foam samples.

I want to take this opportunity to show sincere appreciation to Assoc. Prof. Dr. Esra Erken for giving me the opportunity to use her research lab facilities, and to Ceren Hür, her PhD student, for all of her assistance with the Zeta Potential tests.

My special thanks go to Prof. Dr. Seval Genç, Assist. Prof. Dr. Gül Gülenay Hacıosmanoğlu, and Res. Assist. Serdar Şam from Marmara University for their endless support through this research.

I gratefully acknowledge The Scientific and Technological Research Council of Turkey (TUBITAK) and The Higher Council for Innovation and Excellence of Palestine (HCIE) for their support of this study under the 2521 International Bilateral Research Project (Grant Number: 120N633).

All of my family members deserve my sincere gratitude. I dedicate this thesis to my family in appreciation of harmony and support.

Finally, I want to express gratitude to additional individuals who were not specifically mentioned here.

I dedicate this thesis to my mother Khadro Mohamed, my father Abdi Hashi, my brother Mohamed Abdi and my sisters Naima Abdi and Hodan Abdi who have taught me values and excellence which have allowed me to advance to this stage in my academic career.

TABLE OF CONTENTS

ÖZET

İyonik Fonksiyonel Gruplara Sahip Selüloz Esaslı Adsorbanlarla Ağır Metal İyon Gideriminin Araştırılması

Ağır metal kirliliği, kentsel ve endüstriyel gelişimin artmasıyla tüm dünyada etkisini hissettirmeye başlamıştır. Nehirlerin, göllerin ve diğer su kaynaklarının ağır metal kirliliği, yetersiz su ve atık su arıtımı ve artan endüstriyel faaliyetlerin bir sonucudur. Bu soruna çözüm üretmek amacıyla, son yıllarda, çok sayıda çalışma, su ve atıksuların ağır metal kirliliğinden arındırılması için yeni adsorbanların geliştirilmesine odaklanmıştır.

Bu çalışmada, doğada bol ve yaygın olarak bulunan, ucuz ve erişimi kolay bir kaynak olan selüloz kullanılarak sudaki ağır metalleri tutabilecek iyonik fonksiyonel gruplara sahip yeni bir adsorban malzemenin sentezlenmesi amaçlanmıştır. Adsorban malzemenin üretiminde kullanılacak selülozun yüzeyindeki hidroksil gruplarını daha erişilebilir hale getirmek ve bu sayede selülozun daha reaktif olmasını sağlamak amacıyla sentezlemenin ilk adımında selüloz aktivasyon işlemi uygulanmıştır. PUF sentezinde kullanılan izosiyanat yapısının ağır metal giderim verimine etkisini araştırmak amacıyla, selüloz bazlı poliüretan köpük numunelerinin sentezinde, iki farklı diizosiyanat; alifatik diizosiyanat, 1,6-heksametilen diizosiyanat ve aromatik diizosiyanat, 1,4-fenilen diizosiyanat, kullanılmıştır. Bu yaklaşımla toplam altı farklı selüloz bazlı köpük adsorban sentezlenmiştir. Sentezlenen her köpük örneğinin ağır metal giderim kapasitesinin belirlenmesi için Co^{2+}, Cu^{2+} ve Ni^{2+} iyonları model ağır metal iyonları olarak seçilmiştir. Co^{2+}, Cu^{2+} ve Ni^{2+} sulu çözeltileri kullanılarak , bu tez boyunca AC-HMPUF, AC-PPUF, CAc-PPUF, CAc-HMPUF, CMC-PPUF ve CMC-HMPUF olarak isimlendirilecek olan altı farklı selüloz bazlı adsorban ile Kesikli adsorpsiyon deneyleri gerçekleştirilmiştir. Bu deneylerde, CAc-PPUF'nin, diğer absorban örneklerine göre, 25°C'de, 100 mg/L'lik başlangıç ağır metal konsantrasyonunda, 10 g/L'lik adsorban dozunda ve 6,5'lik pH'ta, 24 saatlik çalkalama süresi sonunda, Co^{2+}, Cu^{2+} ve Ni^{2+} iyonlarını daha yüksek verimle giderdiği gözlemlenmiştir. Belirtilen koşullar altında, bakır, kobalt ve nikel iyonları için CAc-PPUF ile giderim verimleri sırasıyla %62.42, %36.39 ve %23.2 olarak tespit edilmiştir.

CAc-PPUF, Fourier Dönüşümü Kızılötesi Analizi (FTIR), Taramalı Elektron Mikroskobu (SEM), BET yüzey alanı (BET) ve Zeta Potential analizleri ile karakterize

edilmiştir. Önerilen CAc-PPUF yapısı, FTIR analizi ile doğrulanmıştır. SEM görüntüleri, CAc-PPUF'nin değişken mikro gözenek boşluklarına sahip oldukça gözenekli amorf bir yapı olduğunu göstermektedir. CAc-PPUF'un mikrogözenekli yapısı, BET testleri ile incelenmiş ve malzemenin ortalama gözenek yarıçapının 19.96 nm, yüzey alanının ise 23.15 m^2/g olduğu ortaya konmuştur. pH 4-9 aralığında, CAc-PPUF'nin zeta potansiyeli negatif bir yük göstermiştir. Geniş bir pH aralığında zeta potansiyel değerlerinin negatif ölçülmesinin, yüzey fonksiyonel gruplarının Ka değerlerinin düşük olmasına bağlı olabileceği düşünülmektedir. CAc-PPUF'nin zeta potansiyel değerlerinin geniş bir pH aralığında negatif olduğunun belirlenmesi, suda pozitif yüke sahip olan ağır metal iyonlarının uzaklaştırılması için uygun yapıda bir adsorban olabileceğini göstermektedir.

CAc-PPUF'nin ağır metal adsorpsiyonunu tanımlayan uygun izoterm modelini belirlemek için doğrusal olmayan regresyon yöntemi kullanılmıştır. Uygunluğu incelenmek üzere, literatürde adsorpsiyon ile ağır metal giderimi çalışmalarında en yaygın şekilde karşımıza çıkan Langmuir, Freundlich, Sips ve Dubinin-Astakhov izoterm modelleri seçilmiştir. Deneysel veriler istatistiksel olarak model tahminleri ile karşılaştırılarak her bir model tahmini için R^2, $\chi 2$ ve NRMSE değerleri hesaplanmıştır. Seçilen 4 model ile elde edilen istatistiki değerler (R^2, $\chi 2$ ve NRMSE) karşılaştırıldığında 4 modelin de deneysel verilere oldukça yakın tahmin sonuçları verdiği görülmektedir. Freundlich, Sips ve Dubinin-Astakhov modelleri, Cu^{2+} adsorpsiyonu için göreceli olarak biraz daha uygun istatistiki sonuçlar vermektedir. DA modeli, CAc-PPUF üzerine kobalt iyonu adsorpsiyonu için istatistiksel olarak daha iyi tahmin özelliği sergilemektedir. Üç parametreli izoterm modelinin (Sips ve Dubinin-Astakhov), CAc-PPUF üzerindeki Ni^{2+} izotermi için deneysel verilere biraz daha iyi uyduğu gözlemlenmiştir. Freundlich, Sips ve Dubinin-Astakhov modelleri heterojen yüzeye sahip adsorbanlar için uygun modellerdir. CAc-PPUF'nin yüzeyindeki asetat grupları, oksijen atomları ve nitrojen atomları, ağır metal iyonları için bağlanma yerleri olma özelliği taşımaktadırlar. Bu nedenle, CAc-PPUF'nin yüzeyinin heterojen bir yüzey olduğunu söyleyebiliriz. Dolayısıyla bu sonuçlar, CAc-PPUF'nin heterojen doğası ile iyi bir uyum içindedir.

İzoterm deneyleri ayrıca, CAc-PPUF'nin etkinliğinin, çözeltideki ağır metallerin başlangıç konsantrasyonu ile ters orantılı olduğunu göstermiştir. Sudaki ağır metal

başlangıç konsantrasyonu arttığında, giderim veriminin azaldığı gözlemlenmiştir.

CAc-PPUF'nin ağır metal adsorpsiyon hızının belirlenmesi için kinetik deneyler tasarlanmıştır. Bu deneylerde model ağır metal iyonu olarak Cu kullanılmış ve eşit hacimlerdeki 100 ppm Cu^{2+} çözeltileri, farklı zaman aralıklarında, aynı miktarlardaki CAc-PPUF adsorpsiyonuna tabi tutulmuştur. Deneysel verilerin, literatürde yaygın kullanılan üç kinetik model olan yalancı birinci derece (PFO), yalancı ikinci derece (PFO) ve Elovich modelleri ile uyumluluğu yine doğrusal olmayan regresyon yöntemi kullanılarak değerlendirilmiştir. Cu iyonunun CAc-PPUF yüzeyine adsorpsiyon kinetiğinin yalancı ikinci derece (PSO) kinetik modeli ile uyumlu olduğu ve yalancı ikinci derece adsorpsiyon reaksiyonu hız sabitinin de 0.009281 g/(mg.min) olduğu gösterilmiştir.

Suyun pH değerinin CAc-PPUF'nin ağır metal adsorpsiyon kapasitesi üzerine etkisi pH 4.5 - 9 aralığında incelenmiş ve belirtilen aralıktaki pH değişimini ağır metal adsorpsiyon kapasitesi üzerinde istatistiki olarak anlamlı bir fark yaratmadığı tespit edilmiştir. Yine aynı şekilde 15℃, 20℃ ve 25℃'de su sıcaklığının ağır metal adsorpsiyon kapasitesi üzerine etkisine bakılmış, ihmal edilebilir düzeyde olsa da 15℃'deki adsorpsiyon kapasitesinin 20℃ ve 25℃'de elde edilen kapasitelerin az bir farkla üzerinde olduğu görülmüştür. Bu nedenle, CAc-PPUF yüzeyine ağır metal adsorpsiyonunun hafifçe ekzotermik bir reaksiyon olduğu söylenebilir.

CAc-PPUF, Cu iyonlarını verimli bir şekilde adsorbe etmiş ve 1M HCl uygulanarak yapılan rejenerasyon işlemi ile beş döngü desorpsiyon işleminden sonra bile giderim verimi çok fazla azalma göstermemiştir. 5 adsorpsiyon-desorpsiyon döngüsü sonrasında giderim veriminin %79'dan %67.4'e azaldığı gözlemlenmiştir.

Çalışmanın son aşamasında ise yüksek kalsiyum, sodyum, potasyum ve demir iyonları içeren gerçek bir yeraltı suyu örneğinden Co, Cu, Ni, Cr, Pb ve Zn iyonlarının CAc-PPUF ile etkili bir biçimde giderilip giderilemediği test edilmiştir. Yeraltı suyunun CAc-PPUF ile arıtımı Co, Cu, Cr, Pb ve Zn iyonlarının %90'dan fazlasını gidermiştir. Ancak, Ni iyonu giderimi daha düşük seviyede, %51 olarak bulunmuştur. Ni iyonunun gideriminin düşük olmasının nedeni, diğer metal iyonlarının varlığından kaynaklanan rekabet ve sudaki Ni iyonu konsantrasyonunun diğer ağır metallere göre daha yüksek olması ile açıklanabilir.

Çalışma, ilk kez sentezlenmiş olan CAc-PPUF'nin, ağır metal kirliliği içeren suların arıtımında adsorban malzeme olarak etkin biçimde kullanılabileceğini ortaya koymuştur.

Anahtar Kelimeler: ağır metal, selüloz, adsorpsiyon, kobalt, nikel ve bakır, izoterm, PFO, PSO

ABSTRACT

Investigation of Heavy Metal Ion Removal by Cellulose based Adsorbents with Ionic Functional Groups

Heavy metal contamination is spreading throughout the world, especially as urban and industrial development expands. Heavy metal contamination of rivers, lakes, and other water resources has increased as a result of inadequate water and wastewater treatment, and rising industrial activities. To address this problem, numerous studies have concentrated on developing novel adsorbents for the efficient removal of heavy metals from polluted waters.

In this study, we concentrated on the synthesis of a special foam material with particular ionic functional groups utilizing cellulose, a naturally occurring resource that is quite abundant. Synthesis procedures started with the activation of cellulose before its use in the foam formation reaction to make the hydroxyl groups at the surface of the biopolymer more accessible, and thus reactive. In order to investigate the effect of isocyanate structure used for the PUF synthesis on heavy metal removal efficiency, two different diisocyanates; an aliphatic diisocyanate, 1,6-hexamethylene diisocyanate, and an aromatic diisocyanate, 1,4-phenylene diisocyanate, were used for the synthesis of cellulose based polyurethane foam samples. As such, six different cellulose based foam adsorbents were synthesized. Heavy metal removal capacity of each synthesized foam sample was tested for the removal of Co^{2+}, $Cu^{2+,}$ and Ni^{2+} ions as the model heavy metals. Batch adsorption experiments were conducted using six different cellulose based adsorbents, which throughout this thesis are abbreviated as AC-HMPUF, AC-PPUF, CAc-PPUF, CAc-HMPUF, CMC-PPUF and CMC-HMPUF. Batch adsorption experiments at 25 °C for 24 hours demonstrated that CAc-PPUF displayed better Co^{2+}, $Cu^{2+,}$ and Ni^{2+} removal efficiencies at initial heavy metal concentration of 100 mg/L, adsorbent dose of 10 g/L, and pH of 6.5. Under the given conditions, the removal efficiencies were 62.42%, 36.39%, and 23.2% for copper, cobalt, and nickel ions, respectively.

CAc-PPUF was characterized by Fourier Transform Infrared Analysis (FTIR), Scanning Electron Microscopy (SEM), BET surface area (BET), and Zeta Potential analyses. The proposed structure of CAc-PPUF was confirmed by FTIR analysis. SEM exhibits a

highly porous amorphous structure with variable micropore spaces. The mesoporous nature of CAc-PPUF was studied using BET analysis which reveals that the average pore radius of the material is 19.96 nm while the surface area is 23.15 m^2/g. In the pH range of 4–9, zeta potential of CAc–PPUF demonstrated a negative charge. This is attributed to the low K_a values of surface functional groups. Negative zeta potential of CAc-PPUF over a wide pH range makes it a promising adsorbent for the removal of heavy metals since heavy metal ions are positively charged in water.

The isotherm model best suitable for predicting the heavy metal adsorption capacity of CAc-PPUF was identified using the non-linear regression technique. For this purpose, the Langmuir, Freundlich, Sips, and Dubinin-Astakhov isotherm models, which are the most widely used in the literature to simulate the adsorption of heavy metals were selected. By using the experimental observations and the model predictions as constraints, the R^2, $\chi 2$, and NRMSE values for each model prediction were determined. Statistical analysis of each isotherm model prediction revealed that the predictions are highly comparable. Freundlich, Sips, and Dubinin-Astakhov models have slightly better fits for Cu^{2+} adsorption. DA model had statistically better predictions for cobalt ion adsorption onto CAc-PPUF. Three parameter isotherm models (Sips and Dubinin-Astakhov) were observed to show slightly better fits to the experimental data for Ni^{2+} adsorption onto CAc-PPUF. Freundlich, Sips and Dubinin-Astakhov models are described for adsorbents with heterogeneous surfaces. In CAc-PPUF, acetate groups, oxygen atoms, and nitrogen atoms act as binding sites for heavy metal ions. Hence, the surface of CAc-PPUF is heterogeneous. These results, therefore, agree well with the heterogeneous nature of CAc-PPUF.

Isotherm experiments further demonstrated that the heavy metal removal of CAc-PPUF was inversely proportional to the initial concentration of heavy metals in solution. It was found that when the initial concentration of heavy metals in the water increased, the removal efficacy decreased.

Kinetic experiments were designed to determine the heavy metal adsorption rate of CAc-PPUF. In these experiments, Cu was used as the model heavy metal ion and equal volumes of 100 ppm Cu^{2+} solutions were subjected to the same amounts of CAc-PPUF adsorption at different time intervals. The compatibility of the experimental data with

the pseudo-first-order (PFO), pseudo-second-order (PFO) and Elovich models, which are three commonly used kinetic models in the literature, was also evaluated using the nonlinear regression method. It has been shown that the adsorption kinetics of Cu ion on the CAc-PPUF surface is compatible with the pseudo-second order (PSO) kinetic model and the pseudo-second-order adsorption reaction rate constant is 0.009281 g/(mg.min).

The effect of water pH on the heavy metal adsorption capacity of CAc-PPUF was investigated in the pH range of 4.5-9. It was determined that the pH change in the specified range did not make a statistically significant difference on the heavy metal adsorption capacity. Likewise, the effect of water temperature on heavy metal adsorption capacity was examined at 15°C, 20°C and 25°C. The adsorption capacity at 15°C was determined to be somewhat larger than the capacities at 20°C and 25°C, despite the fact that this difference is only minor. As a result, it can be concluded that the heavy metal adsorption reaction on the surface of CAc-PPUF is slightly exothermic.

CAc-PPUF adsorbed Cu ions efficiently, and even after five cycles of desorption with the regeneration process using 1M HCl, the removal efficiency did not appreciably decline. It was shown that after five adsorption-desorption cycles, the removal effectiveness dropped from 79% to 67.4%.

At the last stage of the study, it was tested whether CAc-PPUF could effectively remove Co, Cu, Ni, Cr, Pb, and Zn ions from a real groundwater sample that has high calcium, sodium, potassium, and iron ions. Treatment of the groundwater with CAc-PPUF removed more than 90% of Co, Cu, Cr, Pb, and Zn ions. Ni ion removal, however, was lower, almost 51 %. It could be due to competition caused by the presence of other metal ions, and the substantially higher Ni ion concentration.

The study demonstrated that the newly synthesized CAc-PPUF can be employed successfully as an adsorbent material in the treatment of waters contaminated with heavy metals.

Keywords: heavy metal, cellulose, adsorption, cobalt, nickel and copper, isotherm, PFO, PSO

SYMBOLS

C_e : Equilibrium concentration of metal ion (mg/L)

C_0 : Initial heavy metal ions concentration (mg/L)

Cs : Aqueous solubility (mg/L)

K_1 : The pseudo-first order rate constant

K_2 : The pseudo-second order rate constant

K_f : Freundlich constant ((mg/g)/(mg/L)n)

K_L : Langmuir constant (L/mg)

K_S : Sips constant (mg/L)(-1/nS)

m : Mass (g)

n : Freundlich intensity parameter

nDA : Heterogeneity factor of Dubinin-Astakhov isotherm

qm^S : Maximum Sips adsorption capacity (mg/g)

qe : The mass of metal ion adsorbed per unit mass of adsorbent at equilibrium (mg/g)

Q_{max} : Maximum adsorption capacity (mg/g)

Q_{cal} : calculated amount of metal concentration at equilibrium

Q_{exp} : experimental amount of metal concentration at equilibrium

R^2 : Correlation coefficient

T : Temperature (°C)

T : Time (s)

V : The solution volume (L)

χ^2 : Chi square

Re% : The percent (%) removal efficiency

NRMSE : Normalized root mean square error

α : The initial sorption rate constant (mg/g min)

β : The extent of surface coverage and activation energy

1/n : The heterogeneity factor

ABBREVIATIONS

AAS : Atomic Adsorption Spectrometer

AC : Activated cellulose

AC-HMPUF : Activated cellulose 1,6-hexamethylene Polyurethane foam

AC-PPUF : Activated cellulose 1,4-phenylene Polyurethane foam

Al : Aluminum

As : Arsen

BET : Brunauer-Emmett-Teller (BET)

CAc : Cellulose acetate

CAc-HMPUF : Cellulose acetate 1,6-hexamethylene Polyurethane foam

CAc-PPUF : Cellulose acetate 1,4-phenylene Polyurethane foam

Cd : Cadmium

CMC : Carboxymethyl cellulose

CMC-HMPUF : Carboxymethyl cellulose 1,6-hexamethylene Polyurethane foam

CMC-PPUF : Carboxymethyl cellulose 1,4-phenylene Polyurethane foam

CMF : Carboxymethylated cellulose fiber

Co : Cobalt

Conc. : Concentration

CPUF : Cellulose polyurethane foam

Cu : copper

D-A : Dubinin-Astakhov

EC : Europe Community

EDCs : Endocrine disrupting chemicals

EDHMs : Endocrine-disrupting heavy metals

EPA : Environmental Protection Agency

F : Fluorine

Fig. : Figure

FTIR : Fourier Transform Infrared Spectroscopy

Hg : Mercury

Hg : Mercury

HMs **:** Heavy metals

Mn **:** Manganese

Ni **:** Nickel

NRMSE **:** Normalized root mean square error

Pb **:** Lead

PU **:** Polyurethane

PUF **:** Polyurethane foam

SEM **:** Scanning Electron Microscope

Soln. **:** Solution

Temp. **:** Temperature (^{o}C)

TS **:** Turkish stantard

WHO **:** World Health Organization

Wt. **:** Weight

Zn **:** Zinc

LIST OF FIGURES

LIST OF TABLES

1. INTRODUCTION

1.1. Background

Heavy metals are naturally occurring toxic elements having atomic numbers greater than 20, and elemental density greater than 5 g/cm^3, such as Zn, Cu, Cr, Hg, Pb, Ni, and Co ions. As a result, the term "heavy metals" refers to a total of 51 different elements (López-Botella et al., 2021). Due to their nature, these elements are often found on Earth as trapped ions in silicates or in stable compounds like carbonates, oxides, silicates, and sulfide (Kamil Öden et al., 2022).

Natural processes including volcanic activities, soil erosion, metal corrosion, and geological weathering may result in heavy metal pollution of the environment. Nonetheless, manmade activities now account for the majority of heavy metal contamination. Figure 1.1 shows the major anthropogenic pathways that heavy metals enter the environment. The exponential expansion in the use of heavy metals in various industrial, agricultural, technical, and household activities has resulted in a remarkable increase in human exposure to heavy metals in recent decades. A clear temporal trend toward increased air, water, and soil contamination for a number of heavy metals is reported. Therefore, environmental contamination by heavy metals is one of the major challenges in today's modern society (Srivastava et al., 2017).

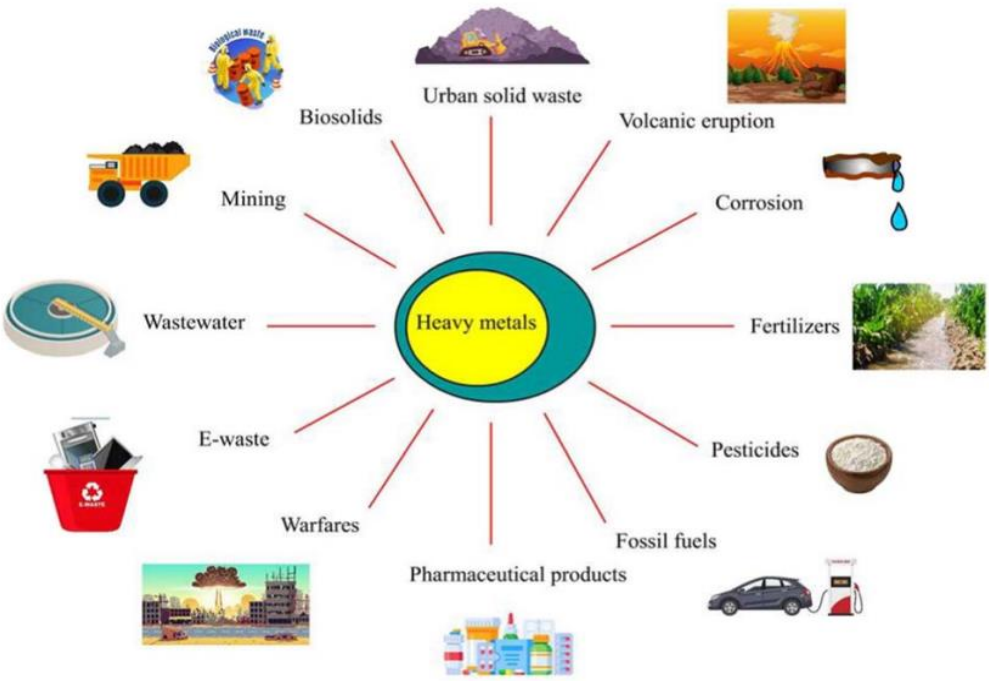

Figure 1.1. The primary anthropogenic pathways that heavy metals enter the environment (Gautam and Chaube, 2018).

1.2. Health Issues Related to Heavy Metal Contamination

It is crucial to stress that human activities that raise the level of environmental contaminants are mostly to blame for the current decline in environmental quality. In today's world, exposure to heavy metals—which can happen through occupational or environmental exposure—poses a risk to reproductive health. Most frequently, exposure to these species comes through tainted food. Exposure to heavy metals results in an accumulation of those substances in the body since the human body lacks the metabolic processes to eliminate them (López-Botella et al., 2021).

The progressive rise in thyroid cancer cases that has been noted globally in recent decades is linked to an increase in environmental exposure to heavy metals, which is a product of the industrialized way of life. Even a slight increase in metal pollution over time due to chronic exposure can have detrimental consequences on many different tissues (Gianì et al., 2021).

They do not break down and are steadily growing in freshwater bodies. Due to their inability to degrade, they bioaccumulate throughout the food chain and have harmful effects at locations far from the pollution source (Kumar et al., 2019).

Heavy metals like lead, arsenic, cadmium, chromium, iron, and vanadium are now frequently linked to water pollution. Even a minute amount of these metals in drinking water could cause unexpected health issues such as brain damage, cancer, and system difficulties (Oyewo et al., 2020). Figure 1.2 shows the adverse effects of frequently observed heavy metals on various human organs.

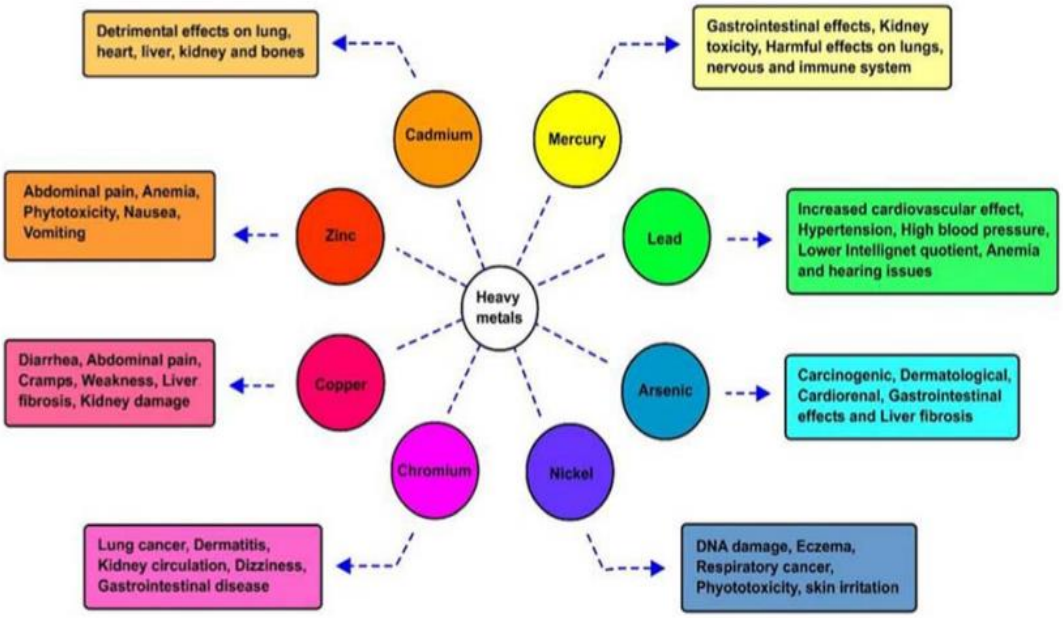

Figure 1.2. Negative impact of frequently observed heavy metals on various human organs (Gautam and Chaube, 2018)

The human central nervous system, brain functioning, and body fluid composition are all adversely affected by heavy metal toxicity, along with the kidney, liver, and other vital organs. Carcinogenesis, Alzheimer's disease, sclerosis, and muscular dystrophy have all been connected to long-term exposure (Azra et al., 2022).

When present in high concentrations, heavy metal ions have been linked to serious adverse health effects such birth defects, cancer, skin sores, growth retardation that causes impairments, and kidney and liver damage. They can also disrupt cellular activity, change enzyme activities, and harm cell membranes (Ezeonuegbu et al., 2021).

1.2.1. Heavy Metals as Endocrine Disrupting Chemicals

Xenoestrogens, also known as endocrine disrupting chemicals (EDCs), are substances that can imitate or block endogenous hormones to interfere with endocrine processes. Previous research has shown that some organic chemicals, mainly those with phenolic or ring structures, can imitate estrogen through their actions on the estrogen receptors. Recent investigations, however, have yielded that heavy metals also imitate the biological action of steroid hormones, such as androgens, estrogens, and glucocorticoids (Dyer et al., 2007). In studies on animals, it was shown that heavy metals like cadmium (Cd), arsen (As), mercury (Hg), nickel (Ni), lead (Pb), tin (Sn), and zinc (Zn) may affect

the endocrine system (Jia et al., 2021).

Due to its affinity for the glucocorticoid receptor and its ability to block the function of glucocorticoids in a number of biological processes, the first metal implicated in endocrine disruption is arsenic (Georgescu et al., 2011).

Metals including aluminum (Al), cadmium (Cd), copper (Cu), and lead (Pb) are categorized as metalloestrogens due to their capacity to obstruct the activity of estrogenic hormones in addition to causing cell damage (Paschoalini et al., 2019).

Since the World Health Organization (WHO) divided EDCs into 11 categories in 2012, the deleterious effects of five heavy metals and their conjugates—arsenic (As), cadmium (Cd), lead (Pb), mercury (Hg), methylmercury, and organotin (tributyltin and triphenyltin)—have gained the most attention (Jia et al., 2021).

Endocrine disruptors like heavy metals interfere with processes that are mediated by endogenous hormones in the body, which has a negative impact on endocrine functions. Heavy metal exposure and male infertility have been linked in some research (López-Botella et al., 2021).

1.3. Heavy metal pollution in aquatic environments

Heavy metals are recognized as significant pollutants of aquatic habitats because of their challenges in metabolism, and tendency to bio-accumulate in the tissues of aquatic animals, particularly fish muscle, which is often consumed around the world as food. Certain metals, including Al, Cu, Cd, and Pb ions, can affect the endocrine systems of fish in addition to harming their cells.

Since water quality changes over time, according to reports, As may accumulate in well water and groundwater derived from natural sources (Georgescu et al., 2011).

Because of the increased demand for freshwater supplies, sometimes inefficient use of water, and escalating pollution, water issues have become a major source of worry on a global scale. In order to manage water resources effectively and maximize economic wellbeing while ensuring social equality and ecological sustainability, a multidisciplinary approach is necessary. In addition to serving as a substitute water source, treated wastewater (TWW) is becoming more and more important as a tool for reducing environmental deterioration (Chfadi et al., 2021).

The main causes of elevated heavy metal concentrations in water bodies are human endeavors like urbanization and industry. The industries that produce electroplating and leather tanning are primarily to blame for the contents of heavy metals (Kumar et al., 2019). Tablel 1.1 shows the effect of Drinking water contaminants from United State Environmental Protection Agency (2018).

Case studies conducted in nations like India show 80% of diseases are waterborne, spreading through contaminated drinking water. Water resources are in low supply as a result of the recent climatic imbalance (Sayyed et al., 2021). Table 1.2 shows a comparison of drinking water guidelines for metal ions concentration (mg/L) from World Health Organization, United State Environmental Protection Agency, Turkish Standard, and Europe community.

Table 1.1. The effect of Drinking water contaminants from EPA (2018)

Metal ion	Drinking water contaminant source	Long-term exposure over the MCL's potential health effects (unless otherwise stated)
Copper	Household plumbing systems corroding and natural deposits eroding.	Temporary exposure intestinal discomfort enduring exposure kidney or liver damage If the action level for copper in their water is exceeded, individuals with Wilson's Disease should speak with their personal doctor.
Lead	Natural deposits are being eroded, household plumbing systems are corroding.	Physical or mental development delays, as well as mild learning disabilities, can occur in infants and young children. Renal problems and high blood pressure for adults.
Mercury	Natural deposit erosion, factory and refinery discharges, landfill runoff, and farmland runoff.	Kidney injury.

Table 1.2. A comparison of drinking water guidelines for metal ions concentration (mg/L) from WHO, USEPA, TS, and EC

Concentration	EPA 2008	WHO guideline 2011	Turkish Standard TS 2005	Europe community (EC) 1998
Copper	1.3	2	2	2
Lead	0.015	0.01	0.01	0.010
Mercury	0.002	0.001	0.001	0.001
Nickel	--	0.02	0.02	0.02

In this study, cobalt, copper, and nickel were selected as target heavy metal ions in contaminated water, due to their ease of measurement.

1.3.1. Cobalt

In trace levels, cobalt is a naturally occurring element found in some ores of the Earth's crust. It is a shiny, silvery blue colored with a density of 8.86 g/cm^3. It can be found in a variety of salts. Pure cobalt is a hard metal, lustrous, steely-gray metal that has no smell (Azra et al., 2022; Rengaraj & Moon, 2002).

Cobalt is a priceless metal with numerous uses in a variety of industrial and medical industries. Cobalt has several uses in the paint, electronics, ceramics, electroplating, metallurgy, food preservation, and cancer treatment industries. It is also used to make vitamin B12 and as a froth stabilizer in beer. Cobalt is a large component of nuclear power plant waste (Aşçi and Kaya, 2014; Azra et al., 2022; Rengaraj and Moon, 2002).

Between 0.05 and 1 mg/L of cobalt is the guideline for the metal in irrigation water and animal wastewater (Azra et al., 2022; Rengaraj and Moon, 2002).

People who have been exposed to cobalt have edema, congestion, and lung hemorrhage as a result of cobalt poisoning. Chronic exposure to cobalt damages the liver and kidney by causing dysfunction, cancer, and genetic mutations, the skin by causing allergic dermatitis, the visceral organs by causing nausea, vomiting, and diarrhea, the respiratory system by causing irritation, asthma, pneumonia, and fibrosis, and the heart by causing heart failure and cardiomyopathy (Azra et al., 2022).

1.3.2. Copper

Despite being regarded as a micronutrient, and one of the frequently utilized heavy metals in the industry, copper is exceedingly hazardous to living things at relatively high levels (Kubra et al., 2021).

According to Kamaruzaman et al. (2017), one form of environmental contamination was water pollution brought on by various companies, including those that produce batteries, paper, fertilizer, pesticides, thermoplastics, galvanizing facilities, and mining operations.

Massive releases of Cu ions into the environment are hazardous to both the environment and human health. Significant health effects are known to occur when exposure levels surpass the authorized upper limit, including cancer, coughing, chronic bronchitis, nausea, impaired lung function, and gastrointestinal discomfort. Menkes syndrome, Alzheimer's disease, Wilson and renal failures are all linked to high copper intake (Kamaruzaman et al., 2017; Kubra et al., 2021).

According to Xie et al. (2018), soil Cu ion criterion of the Europian Union is 140 mg/kg.

1.3.3. Nickel

Nickel is a poisonous, shiny, silvery metal that is not biodegradable with an atomic number of 28. High amounts of nickel exposure can have harmful effects on the body, including birth defects, cancer, respiratory problems, hepatitis, skin rashes, kidney damage, and diarrhea (Ezeonuegbu et al., 2021).

Skin rashes, gastrointestinal problems, and chronic bronchitis can all result from exposure to excessive levels of nickel ions (Qu et al., 2020).

Nickel can be sourced from both artificial and natural sources and is present in all environmental components, including water, soil, and living things. Particle size and weather conditions have a significant impact on the fate of nickel particles in the environment. Most of the time, nickel concentrations for plants above 50 mg/kg are hazardous. Ni levels in fish can range from 0.02-2 mg/kg, and if the water is contaminated, they can go up to ten times higher.

Nickel levels in the air that are often observed range from 5-35 ng/m3, and human exposure levels range from 0.1 to 0.7 g per day. Ni concentration in drinking water is

less than 10 µg/l, whereas it is less than 0.5 mg/kg in fresh food. High concentrations of the metal may be found in soy, various dry vegetables, nuts, and oats. Depending on eating patterns, the daily Ni intake from food ranges from 100 to 800 µg, with a medium intake of 100 to 300 µg. Ni seems to cause pancreatic cell lesions, potentially raising the chance of developing types of diabetes (Georgescu et al., 2011).

Nickel has been utilized in industry for almost a century and is one of the primary elements in the earth's crust. It is primarily found with iron in nature as sulphides, arsenides, and silicates (of lateritic origin) (Kamil Öden et al., 2022).

Stainless steel, nickel-cadmium batteries, and electroplating are all products that are made in the industry by nickel refineries. Electron tubes and the plating business both employ pure nickel. With some metal ions, such as Fe, Cu, Cr, and Zn, it can form alloys (Kamil Öden et al., 2022).

Ni ion concentration in industrial discharges increases as a result of its broad use in the battery production, electroplating, and stainless steel sectors. When the chemicals containing heavy metals 2% or above are discarded after the electroplating process, it causes a global environmental issue(Costa et al., 2022).

Ni ion concentrations in urine from workers in the electroplating sector ranged from 1.74 to 22.73 µg/L (Costa et al., 2022).

The fabrication of stainless steel, storage battery production, casting based on zinc, and electroplating, all involve nickel. Chemical precipitation, electrodialysis, membrane filtration, and activated carbon adsorption are some of the current nickel removal techniques (Yousef et al., 2016).

As reported by Yousef et al. (2016), ion exchange may remove 97% of nickel ions from wastewater.

1.4. Heavy Metal Removal Techniques

Heavy metal pollution of aquatic environments is a major issue because of their potential toxicity and accumulation in aquatic habitats. They come from a variety of anthropogenic and natural sources. Metal pollution in freshwater environments can happen as a direct result of atmospheric precipitation, as a result of geologic weathering, or as a result of effluent from home, municipal, or industrial wastewaters. Wastewater

produced by a variety of industries, including metallurgy, mining, chemicals, paints, metal coatings, textile dyes, tanneries, batteries, construction, and shipping contain high levels of heavy metals (Es-Sahbany et al., 2019). Therefore, the removal and/or reduction of the amount of certain heavy metals to the acceptable levels by the standards prior to discharge into aquatic environments is required for the protection of surface water quality (Es-Sahbany et al., 2019).

Several traditional and cutting-edge technologies have been introduced to address heavy metal removal from wastewater and contaminated water. Although they have been extensively employed, traditional water treatments like oxidation, electro-precipitation, membrane separation, coagulation-flocculation, evaporation, floatation, and ion exchange are frequently insufficient for effective water treatment (Sayyed et al., 2021). Techniques such as membrane separation, adsorption, absorption, flocculation, filtration, chemical precipitation, and ion exchange are all effective ways to remove heavy metals contamination in water. Due to its simplicity, affordability, and faster rate of pollution removal, the adsorption method is more competitive than other procedures. Since it is also ecologically beneficial, adsorption is frequently used as a low-cost, and highly successful method of addressing heavy metal contamination (Ding et al., 2023; Sayyed et al., 2021). Wastewater treatment has traditionally relied heavily on activated carbon adsorption. The activated carbon process, however, is not energy effective, and is therefore not cost effective. The development of economical, energy-saving, environment-friendly, adsorption-based water treatment systems using biocompatible, biodegradable raw materials such starch, cellulose, and chitin has therefore recently attracted increasing research interest (Sayyed et al., 2021). The most frequent technique for creating unique structures on the basis of base materials adsorbents is chemical modification. Generally, natural polymers are preferred as base materials due to their plentiful supply, low cost, direct modification, non-toxicity, and ease of degradation (Liu et al., 2022). Since cellulose is naturally abundant, easily accessible, and has unique physicochemical features associated with its specific structure, cellulose-based adsorbent materials are frequently investigated, and proven to be more effective than other adsorbent materials (Kausar et al., 2023).

1.5. Cellulose

Cellulose serves as the foundation for the cell walls of green plants. It is a linear chain of thousands of connected D-glucose units that makes up the polysaccharide. Additionally, it is non-toxic, effordable, and biodegradable (Oyewo et al., 2020). It is the most prevalent and easily available renewable polymer on the planet. Around 33% of all plant materials are made of cellulose, with cotton making up 90% and wood 40-50% (Kausar et al., 2023). Cellulose is a white substance that has no flavor or smell. In addition to being the richest biopolymer in the world, cellulose is renewable, biodegradable, and a neutral fabric (Sayyed et al., 2021). Each hydro-glucose unit of cellulose contains three OH groups, each of which carries several active sorption sites that increase the capacity to remove contaminants from wastewater. It has a low solubility in most organic solvents and is hydrophobic (Sinha et al., 2023). The two functional groups in cellulose are hydroxyl and methylol (in each unit). Due to the absence of branching and side chains, it has an ordered structure. There are two types of OH groups in cellulose; i) the main OH in the methylol group at carbon number six, and ii) secondary OH groups at carbons three and four (Kausar et al., 2023). Figure 1.3 shows the Structure of cellulose.

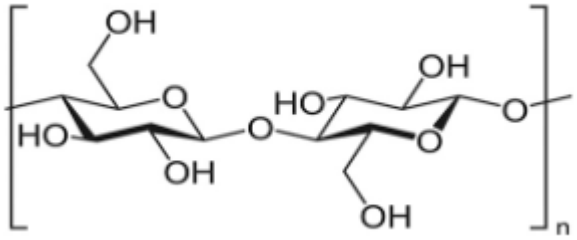

Figure 1.3. The Structure of cellulose (Kausar et al., 2023).

In comparison to their counterparts without the chemical change, the modified materials have significant adsorption capabilities. The adsorption capacity of cellulose-based adsorbents is increased by chemical alterations, which functionalize the adsorbent's surface and produce futher active binding sites for an efficient adsorption rate of the adsorbate (Kausar et al., 2023). It is crucial to remember that the majority of currently used adsorbents are typically changed by single functional groups, such as -CN, -SH, amino groups, sulfate, xanthate, and others (Liu et al., 2022). In most instances, cellulose must be chemically modified in order to create new sustainable goods (Oyewo et al.,

2020).

One of the main byproducts of cellulose, which is colorless, non-toxic, odorless, and soluble in water, is carboxymethyl cellulose (CMC). The structure of CMC hydrogels has several hydroxyl and carboxyl groups, which have been employed as adsorbents to remove metal ions (Sun et al., 2022).

1.6. Polyurethane

At IG Farben in Germany, Otto Bayer and his coworkers produced the first polyurethane (PU) in 1937 (Dutta, 2018). Several fundamental ingredients, such as polyisocyanate(s), catalyst(s), polyol(s), and blowing agent(s), must be stirred in order to create polyurethane foams (PUF) (Furtwengler et al., 2017). Alcohols carrying two or more reactive hydroxyl (-OH) groups in each molecule such as diols or triols, and isocyanates with multiple reactive isocyanate groups (-NCO) in each molecule (polyisocyanates, diisocyanates) undergo condensation processes (Dutta, 2018). Figure 1.4 shows the reaction of Polycondensation.

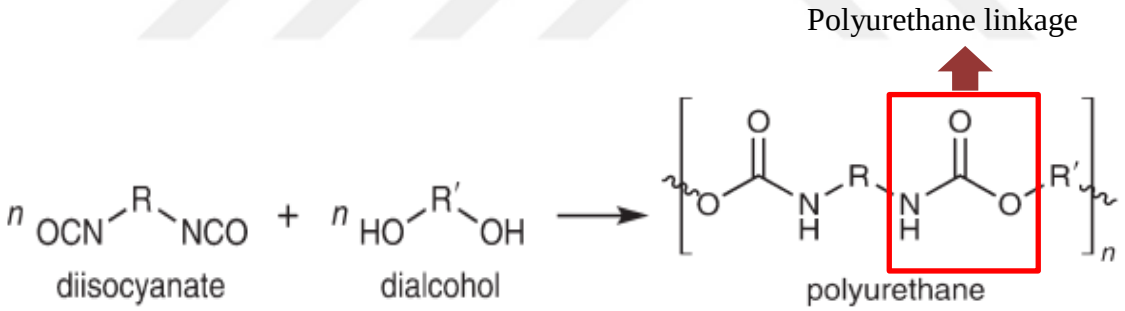

Figure 1.4. The reaction of Polycondensation (Pinto, 2010).

Foams are adaptable polymeric materials which can be categorized as flexible, semi-rigid, or rigid depending on their mechanical performance characteristics and densities (Carriço et al., 2016).

One of the major polymer families is polyurethane (PU), with annual production reaching 18 million tons in 2016 and 11, 2.2, and 0.2 million tons in 2017 for polyether, polyester, and biobased polyol, respectively. and ranking the manufacture of PUs at number six globally (Furtwengler et al., 2017).

The versatility of urethane chemistry and the inventiveness of polymer scientists are

demonstrated by the uses of polyurethane as coatings, foams, fibers, and elastomers.

Condensation of a polyisocyanate and a polyol occurs during the polymerization step to create polyurethanes (Pinto, 2010).

The production of sustainable and environmentally friendly materials has been studied using polyurethane foams made from bio-based polyols (Carriço et al., 2016).

2. MATERIALS AND METHODS

2.1. Materials

2.1.1. Chemicals and reagents

All reagents and chemicals used in this research were analytical grades. Ultra pure water was used for the preparation of all the standard solutions throughout the study. 1000 ppm, high purity, $Cu(NO_3)_2$, $Co(NO_3)_2$, and $Ni(NO_3)_2$ stock AAS calibration standards, accredited to ISO/IEC 17025, and ISO 17034 were purchased from Sigma-Aldrich (Germany). Nitric acid, HNO_3 (Spectrosol®, England) (65%), high purity standards to prepare target heavy metal standard it was mainly used Sigma Aldrich.

The common apparatus which were used during this research contains Erlenmeyer flask, volumetric flask, beakers, reagent plastic bottle, centrifuge tube, test tube rocks, magnetic stirrer, funnel, mortar and pestle, wash bottle, syringe, PTFE filter, graduated cylinder, spatulas and digital balance.

100 ppm stock aqueous Cu^{2+}, Co^{2+}, and Ni^{2+} test solutions were prepared by dissolving an appropriate mass of $CuSO_4.5H_2O$ (CAS-No: 7758-99-8 purchased from Sigma Aldrich (Germany)), $CoCl_2.6H_2O$ (CAS-No: 7791-13-1 purchased from Sigma Aldrich (Belgium)), and $NiSO_4.6H_2O$ (CAS-No: 10101-97-0 purchased from and Sigma Aldrich (Germany)), respectively. Stock solutions were prepared in adequate ratios to prepare the test solutions having 20, 40, 60 and 80 ppm heavy metal concentrations.

2.1.2. Instrumentation

All the instruments that were used in this study are: Malvern Zetasizer (Nano ZS90, UK), pH meter (Tethys EL300, France), shaker (IKA 15 to 500 rpm Digital Speed Control, Germany), FT/IR-4700 spectrometer (Jasco, Japan), BET (AUTOSORP-1C/MS), QUANTA 400F Field Emission (SEM) and Perkin Elmer AAnalyst 400 Atomic Absorption Spectrometer.

2.2. Methods

2.2.1. Synthesis of Foam samples

2.2.1.1. Activation of cellulose

Cellulose is generally subjected to an activation step before it is submitted to a chemical

reaction. Otherwise, the reaction product might be unpredictable or irreproducible. This is because the availability of the hydroxyl groups at the surface of the biopolymer are more accessible for a chemical reaction than those in the crystalline region (Heinze et al., 2018). Therefore, in this study cellulose was initially activated before its use in a chemical reaction. 1.0 g of cellulose was added to 50 mL of distilled water in a round-bottomed flask. The contents were mixed for 120 minutes at room temperature. The water part was separated by vacuum filtration, and 50 mL of methanol was added into the flask. Cellulose/methanol mixture was stirred for one hour. After stirring, methanol was separated by vacuum filtration. Addition, stirring, and separation of methanol was repeated 3 times. In the final step of the activation process, cellulose was left in 50 mL of N,N-dimethyl acetamide (DMAc) overnight. The activated cellulose (AC) was separated from DMAc by vacuum filtration.

2.2.1.2. Formation of AC gel

27 mL of DMAc containing 2.4 g LiCl was mixed with activated cellulose in a round-bottomed flask. The contents was mechanically mixed with magnetic stirrer at room temperature until a clear gel was obtained (approximately 3 hours).

2.2.1.3. Preparation of AC based polyurethane foam

As discussed earlier, polyurethane foam (PUF) can be synthesized using different isocyanates for the polycondensation reaction. In order to investigate the effect isocyanate structure used for the PUF synthesis on heavy metal removal efficiency, in this study, two different diisocyanates; an aliphatic diisocyanate, 1,6-hexamethylene diisocyanate, and an aromatic diisocyanate, 1,4-phenylene diisocyanate, were used for the synthesis of cellulose based polyurethane foam samples.

2.2.1.3.1. Preparation of AC based polyurethane foam using 1,6-hexamethylene diisocyanate

Half of the produced gel was mixed with 1mL of 1,6-hexamethylene diisocyanate in a beaker, followed by the addition of 0.5 mL tetrahydrofuran (THF), and a catalytic amount of (0.1 mL) diisopropyl amine. The contents were mixed for 60 minutes at room temperature. Then, a few drops of water were added. The resulting foam, AC-HMPUF, was washed with 100 mL of distilled water several times, filtered, and dried at 60°C for

one hour. Figure 2.1 shows the synthesis reaction of AC-HMPUF.

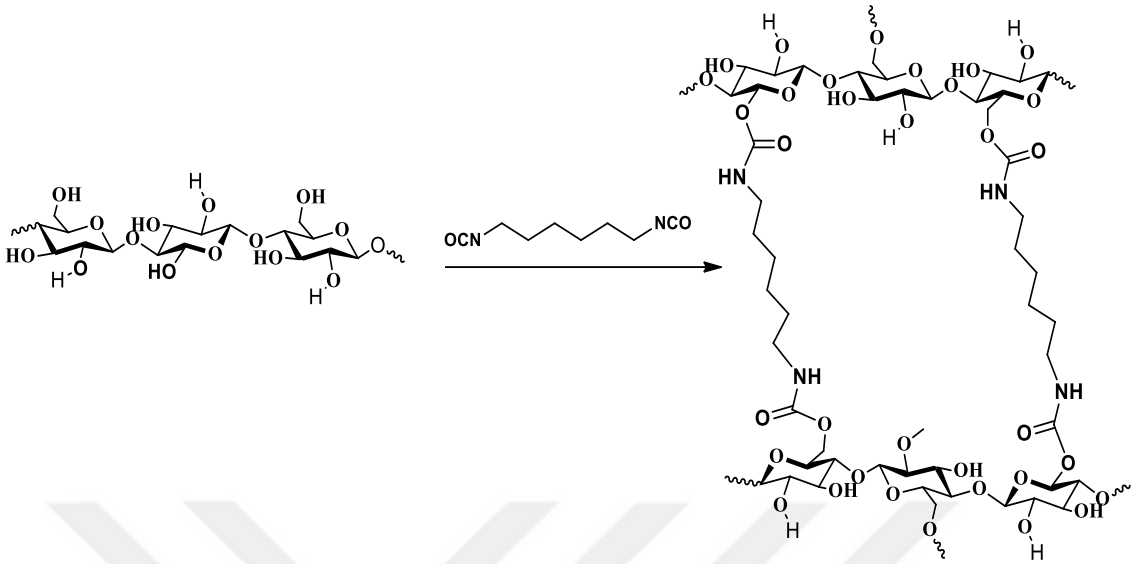

Figure 2.1. Synthesis of AC-HMPUF

2.2.1.3.2. Preparation of AC based polyurethane foam using 1,4-phenylene diisocyanate

1g of 1,4-phenylene diisocyanate, 0.5 mL of THF, and a catalytic amount of (0.1 mL) diisopropyl amine were separately added to the other half of the gel. The contents were mixed for 60 minutes at room temperature. Then, a few drops of water were added. The resulting foam, AC-PPUF, was washed with 100 mL of distilled water several times, filtered, and dried at 60°C for one hour. Figure 2.2 shows the synthesis reaction of AC-PPUF.

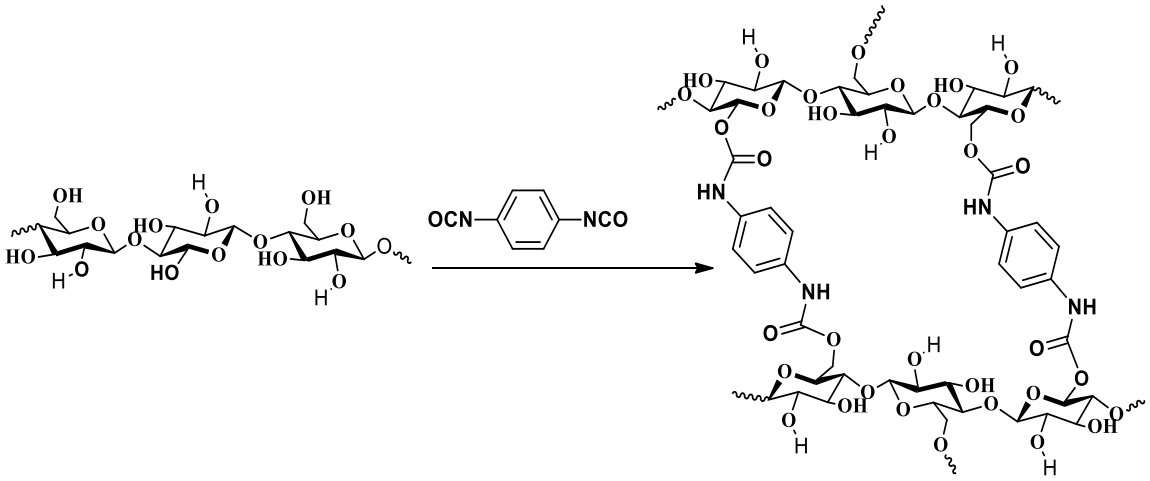

Figure 2.2. Synthesis of AC-PPUF

2.2.1.4. Preparation of carboxymethyl cellulose

Chemical modification of cellulose is essential to improve its reactivity by increasing the accessibility of the hydroxyl groups. Carboxymethyl cellulose (CMC) is a derivative of cellulose having carboxymethyl groups (-CH2-COOH) bound to some of the hydroxyl groups of cellulose. Carboxymethylation is a well-known technique for chemical modification of cellulose (Heinze et al., 1999). A totally homogeneous carboxymethylation of cellulose dissolved in isopropyl alcohol is possible with sodium monochloroacetate, and an aqueous solution of NaOH. For this purpose, 10 g of cellulose was dissolved in 150 mL of isopropyl alcohol under nitrogen, in a three necked round-bottomed flask equipped with a condenser, a magnetic stirring bar, and a thermometer.15 mL of distilled water was added to the reaction mixture followed by the addition of 12 of mL 50% aqueous NaOH solution dropwise through the septum using a syringe over a period of 10 minutes. 50 mL of isopropyl alcohol was then added. A 14.5 mL suspension of sodium chloroacetate was added to the mixture (in one portion). The mixture was heated gradually to 60 °C over an hour, and maintained at 60 °C for another 1 hour. 8g of acetic acid was then added to the mixture. The product, CMC, was collected by suction filtration and washed 3 times with a solution of methanol and water (120:40 mL), respectively. Then, the product was washed with 100 mL of methanol only and dried at room temperature. Figure 2.3 shows the synthesis reaction of CMC.

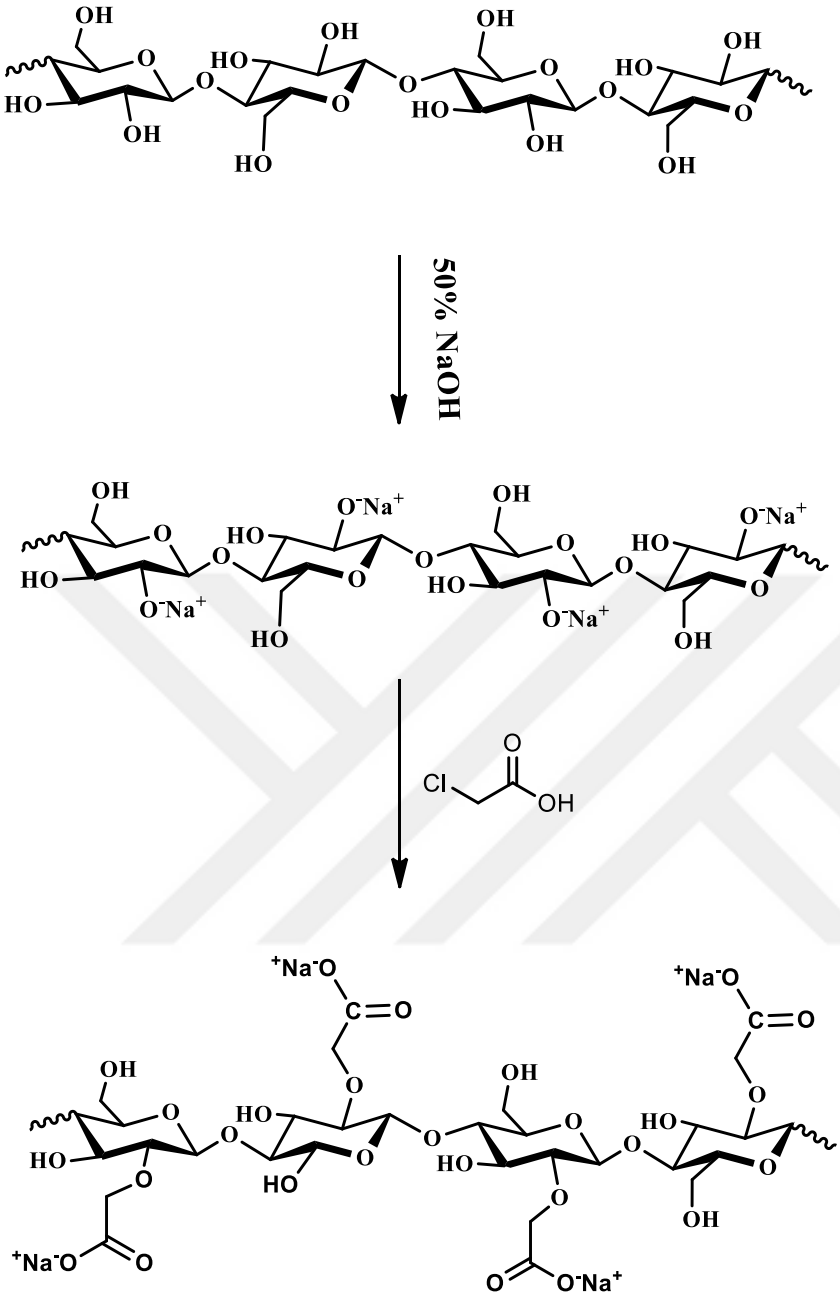

Figure 2.3. Synthesis of CMC

2.2.1.4.1. Preparation of CMC based polyurethane foam using 1,6-hexamethylene diisocyanate

1g of CMC, synthesized as described above, was mixed with 1 mL of distilled water and stirred in a beaker for 30 minutes until a clear gel was obtained.10 mL of DMAc was added to the gel followed by the addition of a catalytic amount of (0.1 mL) diisopropyl amine. An excess amount of 1,6-hexamethylene diisocyanate (3mL) was then added. The contents were mixed for 60 minutes at room temperature, then a few drops of water

were added. The resulting foam, CMC-HMPUF, was washed with 100 mL distilled water several times, filtered, and dried at 60°C for one hour. Figure 2.4 shows the synthesis reaction of CMC-HMPUF.

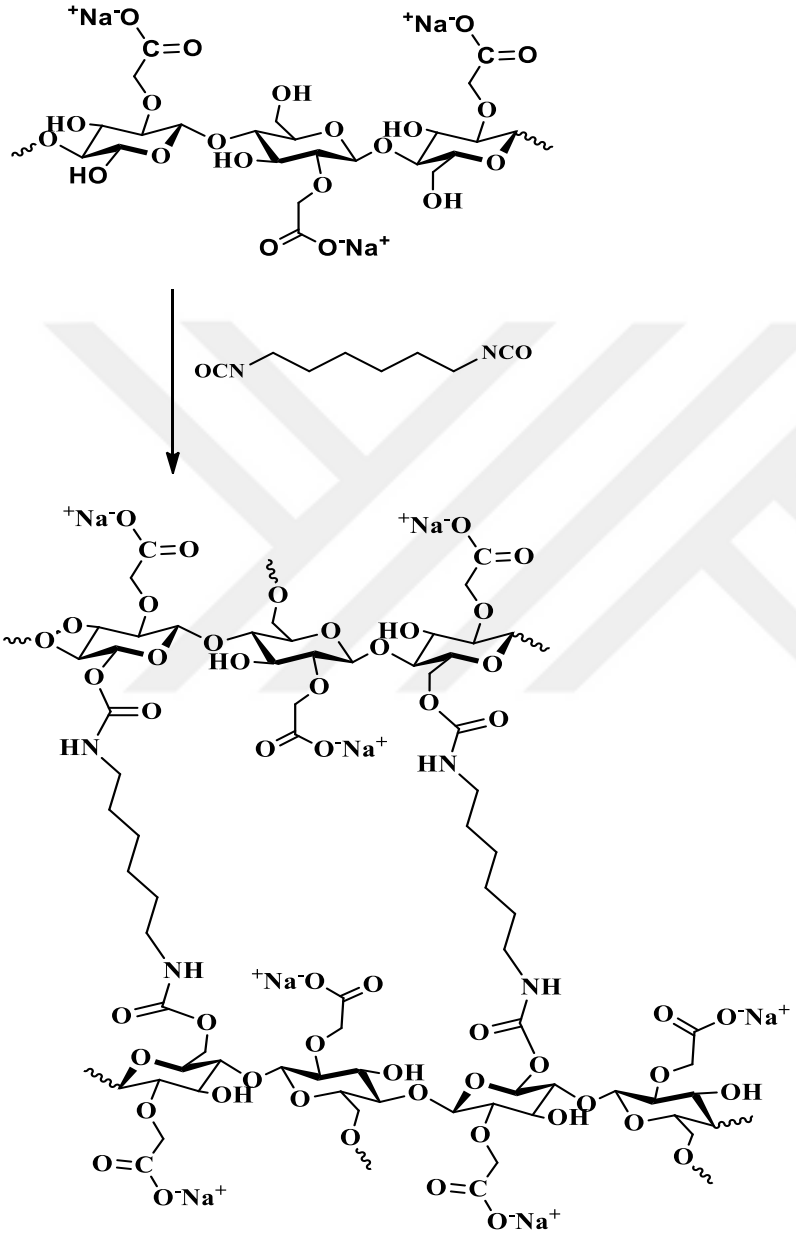

Figure 2.4. Synthesis reaction of CMC-HMPUF

2.2.1.4.2. Preparation of CMC based polyurethane foam using 1,4-phenylene diisocyanate

1g of CMC was added to 1 mL of distilled water. The mixture was stirred in a beaker

for 30 minutes until a clear gel was obtained. 1 g of 1,4-phenylene diisocyanate dissolved in 10 mL of DMAc was added to the gel followed by the addition of a catalytic amount of (0.1 mL) diisopropyl amine. The contents were mixed for 60 minutes at room temperature, then a few drops of water were added. The resulting foam, CMC-PPUF, was washed with 100 mL of distilled water several times, filtered, and dried at 60°C for an hour. Figure 2.5 shows the synthesis reaction of CMC-PPUF.

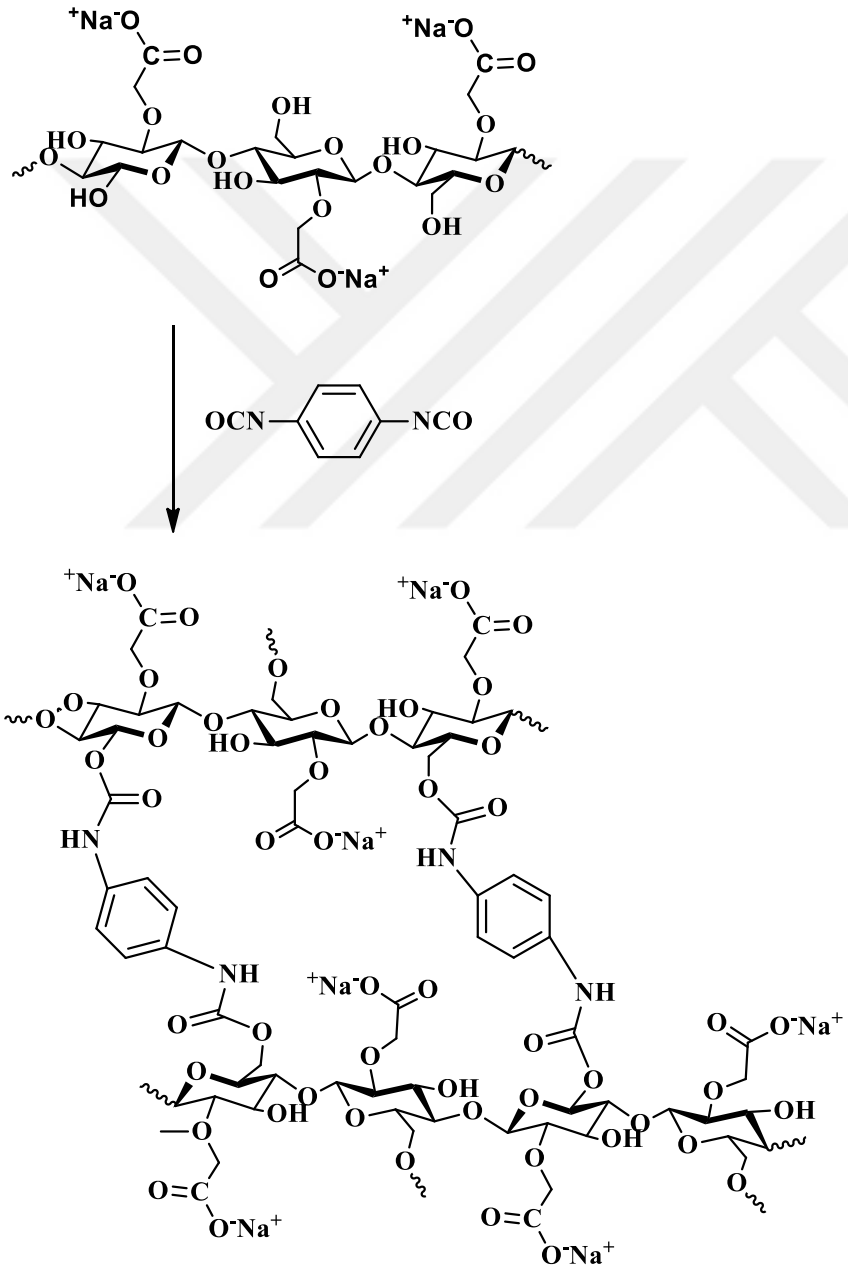

Figure 2.5. Synthesis of CMC-PPUF

2.2.1.5. Preparation of Cellulose Acetate

During production of cellulose acetate, 5 g of cellulose was first dissolved in 50 mL of acetic acid in a flask with two necks, round bottom, a condenser, and a magnetic stirring bar, and a thermometer. The solution was mixed for one hour under nitrogen to activate cellulose before reacting with acetic anhydride. Then, 1.20 mL of H_2SO_4 as a catalyst was added to the solution. The content was stirred in ice bath until the mixture temperature reached to 0 ℃. After that, 30 mL of acetic anhydride was added into the flask. The mixture was gradually heated to 50℃ over an hour. The temperature was then maintained at 50 °C for another one hour. The product, cellulose acetate, CAc, was collected by suction filtration, washed three times with water, and dried at room temperature. The synthesis reaction of CAc thus produced is presented in Figure 2.6.

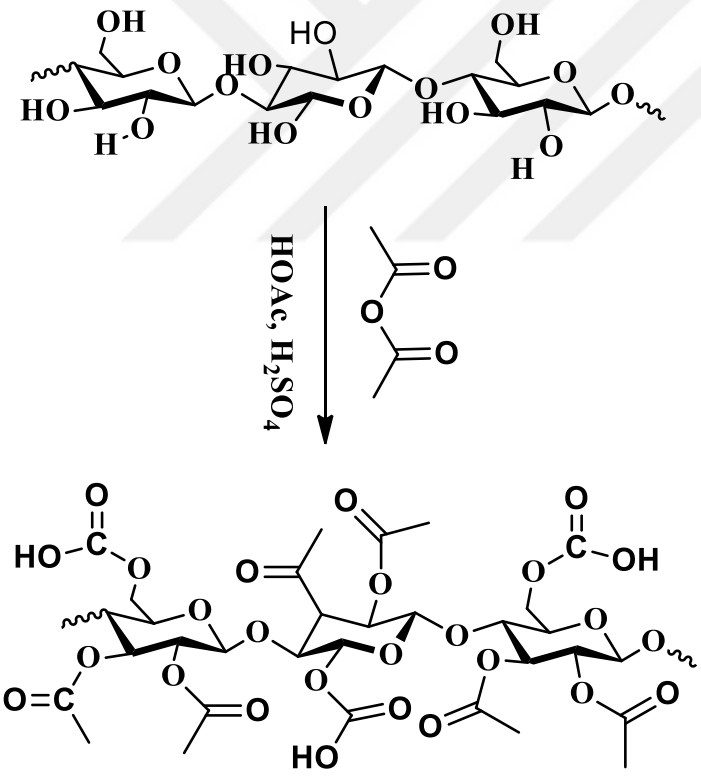

Figure 2.6. Synthesis of CAc

2.2.1.5.1. Preparation of CAc based polyurethane foam using 1,6-hexamethylene diisocyanate

2.0 g of CAc was dissolved in 50 mL of DMAc. The contents were mixed for 120

minutes at room temperature until a clear gel was obtained. Half of the produced gel was mixed with 1 mL of 1,6-hexamethylene diisocyanate in a beaker, followed by the addition of 0.5 mL THF and a catalytic amount of (0.3 mL) diisopropyl amine. The contents were mixed for 60 minutes at room temperature, then a few drops of water were added. The resulting foam, CAc-HMPUF was washed with 100 mL of distilled water several times, filtered, and dried at 60°C for an hour. Figure 2.7 shows the synthesis reaction of CAc-HMPUF.

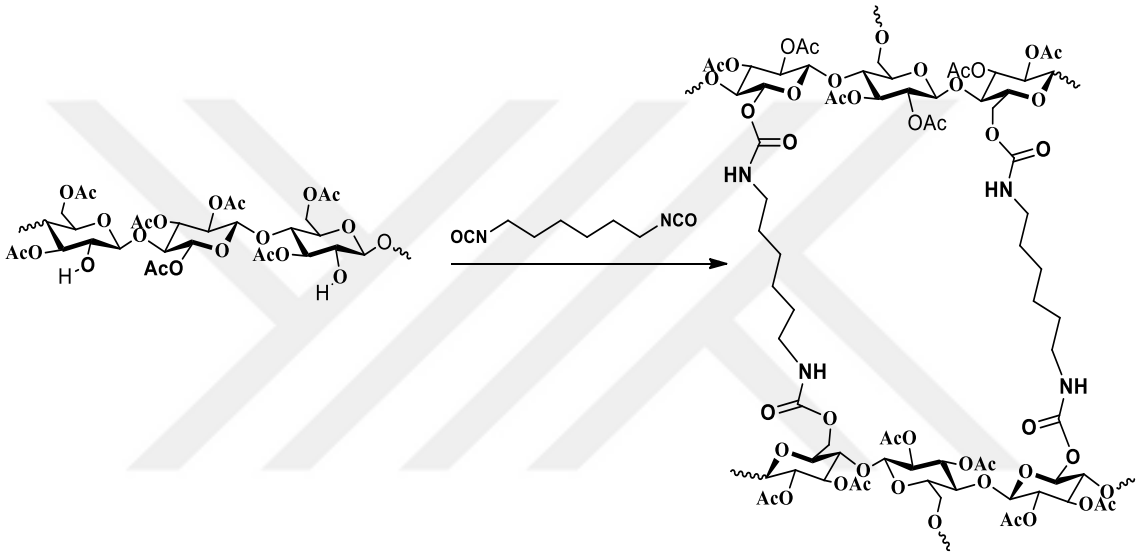

Figure 2.7. Synthesis of CAc-HMPUF

2.2.1.5.2. Preparation of CAc based polyurethane foam using 1,4-phenylene diisocyanate

1g of 1,4-phenylene diisocyanate was added to the other half of the produced gel in a beaker, followed by the addition of 0.5 mL THF and a catalytic amount of (0.3 mL) diisopropyl amine. The contents were mixed for 60 minutes at room temperature, then a few drops of water were added. The resulting foam, CAc-PPUF was washed with 100 mL of distilled water several times, filtered, and dried at 60°C for an hour. Figure 2.8 shows the synthesis reaction of CAc-PPUF.

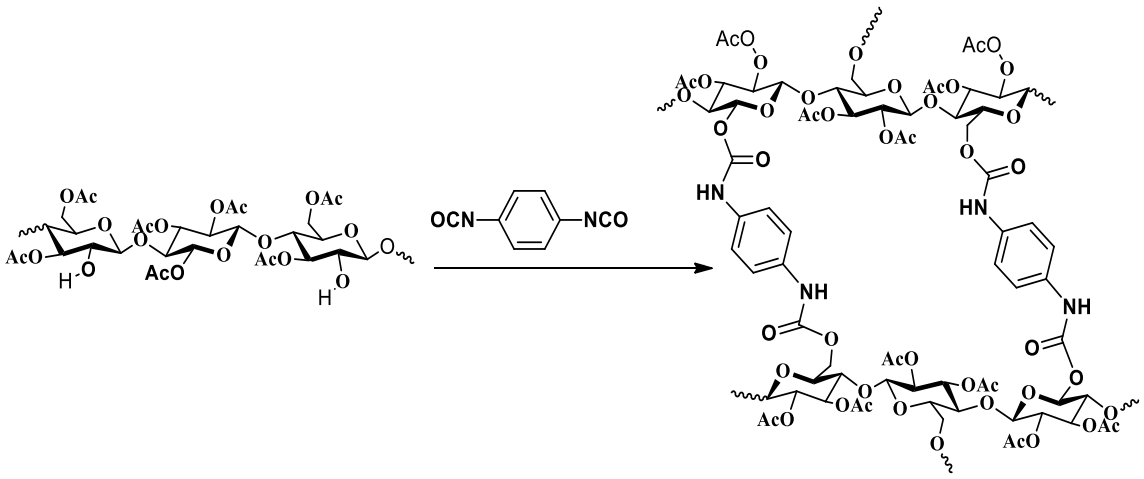

Figure 2.8. Synthesis of CAc-PPUF

2.2.2. Material characterization

Fourier transform infrared (FTIR) spectrometry was employed to analyze the functional groups of CAc-PPUF adsorbent. FTIR spectra were recorded on Jasco Japan 4700 FTIR spectrometer (wave number range of 4000-500 cm^{-1}) as shown in Figure 3.2.

Brunauer-Emmett-Teller (BET) was conducted to analyze surface area of CAc-PPUF foam material. The specific surface area (m^2/g) of adsorbents is one of the most important characteristics because it has a high influence on the adsorption performance. The surface area was determined using N_2 and CO_2 adsorption and desorption isotherms (Mukhtar et al., 2020a).

Yurdakal et al., (2019) reported that the Brunauer-Emmett-Teller (BET) model is the most common to assess isotherms describing a multilayer adsorption. BET was examined using (AUTOSORP-1C/MS), (BET).

2.2.2.1. Zeta Potential

0.1 g/L of adsorbent (CAc-PPUF) mixture was prepared in 20 mL of 0.1 M NaCl solution. Then, the pH of the mixture was adjusted to the desired pH in the range of 4 to 9 by the addition of appropriate amount of 0.1 M NaOH or 0.1 M HCl. In order the surface reactions to reach to equilibrium, all the adsorbent samples were shaken for 24 hours. The Zeta potentials of the mixtures were then measured by Malvern Zetasizer (Nano ZS90, UK).

2.2.3. Batch Adsorption Experiments

Studies on adsorption were conducted in an IKA (Germany) temperature controlled shaker in batch mode at 25 ℃ for 24 hours unless otherwise noted with a mixing speed of 200 rpm. After the adsorption process, the samples were filtered with 0.2 μm PTFE filter. Then, the remaining heavy metal concentrations were measured by atomic absorption spectroscopy using a Perkin Elmer AAnalyst 400 spectrometer. In order to assess the adsorption capacity, the mass of heavy metal ion adsorbed per unit mass of foam material was calculated using Equation 2.1. Some pictures taken during the experiments is presented in Figure 2.9.

$$q_e = \frac{(C_0 - C_e)V}{m} \tag{2.1}$$

In Equation 2.1, C_0 and Ce are the initial and equilibrium concentrations of heavy metals (mg/L), q_e is the mass of pollutant adsorbed per unit mass of adsorbent (mg/g), V is the solution volume (L) and m is the adsorbent mass (g).

The percent (%) removal efficiency was calculated using Equation 2.2.

$$Re\% = \frac{(C_0 - C_e)}{C_0} \text{x} 100\% \tag{2.2}$$

where Re% is the percent removal efficiency.

Figure 2.9. Some pictures were taken during the experiments.

2.2.3.1. Effect of pH

In order to see the effect of pH on heavy metal adsorption capacity of CAc-PPUF, several 10 mL of 60 ppm of Cu aqueous solutions were prepared, and CAc-PPUF was added at 0.1 g/L concentration. The pH of each mixture was adjusted to the desired pH in the range of 4 to 9 by the addition of appropriate amount of 0.1 NaOH or 0.1 HCl. Batch adsorption experiments were carried out as described in Section 2.2.3.

2.2.3.2. Effect of temperature

The effect of temperature on the removal of copper ion in aqueous solution by CAc-PPUF were examined at three different temperatures of 15℃, 20℃ and 25℃. The initial concentration was investigated in the range of 20-100 mg/L by keeping the adsorbent dose constant. Batch adsorption experiments were carried out as described in Section 2.2.3.

2.2.4. Desorption and Reuse Experiments

Cost of heavy metal removal by adsorption onto CAc-PPUF can be significantly reduced if the spent CAc-PPUF can be regenerated, and reused. Therefore, in this section, the reuse potential of CAc-PPUF by an appropriate desorbing agent is explored. According to Liu et al. (2001), only 7.2% of the adsorption capacity is lost after 30 repetitions of the adsorption and desorption cycles, and the Cu^{2+} ions that have been adsorbed on a cellulose-based adsorbent may be recovered with HCl aqueous solution with a recovery rate of 62–100%. Therefore, in this study, in order to examine the regeneration and reuse potential of CAc-PPUF, 1 M HCl solution was used as described by (Liu et al., 2002). Into 10 mL of 60 ppm aqueous Cu solution, CAc-PPUF was added as the adsorbent material. Batch adsorption experiment was carried out as described in Section 2.2.3. After the adsorption process, the Cu-loaded CAc-PPUF was separated by centrifugation. Aqueous part was removed, and analyzed for the remaining Cu^{2+} ions. Desorption was carried out by adding 10 mL of 1 M HCl to the Cu-loaded CAc-PPUF, and agitating the mixture for an hour. Then the mixture was centrifuged, and the acid solution was separated. The regenerated CAc-PPUF was washed several times with deionized water by centrifugation and filtration, and dried overnight under vacuum at 40 ℃. CAc-PPUF, after being regenerated, was reused for further Cu^{2+} adsorption. The adsorption-

desorption experiments were repeated for five cycles. % Cu ion removal efficiencies were calculated for each cycle.

2.2.5. Validation of kinetics and isotherm models

In this study, nonlinear method was conducted for estimating the equilibrium and kinetic parameters of adsorption since the linear method is limited to two variable equations. Non-linear method, on the other hand, can provide solutions for more complex sorption isotherm and kinetic models (Dubey et al., 2016). Nevertheless, nonlinear optimization gives a mathematically rigorous method for calculating parameter values with a small number of error analysis techniques (Yousef et al., 2016). Nevertheless, nonlinear optimization gives a mathematically rigorous method for calculating parameter values with a small number of error analysis techniques (Yousef et al., 2016).

The models were assessed using the Chi square (χ^2), correlation coefficient (R^2), and normalized root mean square error (NRMSE) in order to determine how well the equations fit the experimental data. Table 2.1 provides the equations required to calculate these models.

Error function analysis

Non-linear regression analysis

Non-linear regression was applied to analyze all of the model parameters using Microsoft Office Excel software (Microsoft Corp., USA). To assess the accuracy with which the equation fits the experimental data, the optimization technique needs an error function to be established. The residual root mean square error (RMSE), the chi-square test, and the correlation coefficient (R^2) were also employed to assess the goodness-of-fit (Vijayaraghavan et al., 2006).

Table 2.1. Parameters used for model evaluation (Jasper et al., 2020; Vijayaraghavan et al., 2006).

Parameter	Equation
Chi square	$\chi^2 = \sum_{i=1}^{n} \frac{(q_{exp} - q_{calc})^2}{q_{calc}}$
Correlation coefficient	$R^2 = 1 - \frac{\sum_{i=1}^{n} (q_{exp} - q_{calc})^2}{\sum_{i=1}^{n} (q_{exp} - q_{exp,mean})^2}$
Normalized root mean square error	$NRMSE = \frac{\sqrt{\frac{\sum_{i=1}^{n} (q_{exp} - q_{calc})^2}{n}}}{q_{exp,max} - q_{exp,min}}$

Where n is number of data points; q_{exp} and q_{calc} are the quantities adsorbed determined experimentally and the quantities adsorbed calculated by the models, respectively; $q_{exp,min}$, $q_{exp,mean}$ are the maximum, minimum and mean values of the quantities adsorbed determined experimentally, respectively.

The effective model gives R^2 close to the unity where NRMSE and χ^2 are close to zero. It demonstrates that the proposed model equation is capable of effectively predicting experimental data.

2.3. Preparation of Standard Solutions

AAS calibration standard solutions were prepared by firstly diluting the 1000 ppm stock solutions of Cu^{2+}, Co^{2+}, and Ni^{2+} to 100 ppm of medium stock in separate volumetric flasks by the addition of 2% HNO_3. The medium stock solution was further diluted with 2% HNO_3 to the desired concentrations for the calibration standards, in the range of 1-5 mg/L.

2.4. Heavy metal analysis

Perkin Elmer AAnalyst 400 Atomic Absorption Spectrometer instrument was used to conduct the calibration and concentration determination of Copper, Cobalt, and Nickel.

Linearity acceptance criteria was set as coefficient of determination (R^2) greater than or equal to 0.995. In this experiment the three preliminary adsorption experiments, Cu^{2+} showed higher than the target whereas Co^{2+}, Ni^{2+} was found almost equal to 0.995. Calibration curves for Cu^{2+}, Co^{2+}, and Ni^{2+} are given as supporting information in Appendix A.

2.5. Determination of Heavy Metal Removal Capacities of Each Synthesized CPUF

Aqueous solutions of Cu, Co, and Ni ions were prepared at 100 mg/L initial concentration. 0.1 g of each adsorbent material was added into a flask containing 10 ml aqueous heavy metal solution. The pH of all test solutions were 6.5. Batch adsorption experiments were carried out as described in Section 2.2.3.

2.6. Adsorption Isotherm Studies of Heavy Metals with the Selected CPUF

10 mL of aqueous heavy metal solutions at 20, 40, 60, 80, and 100 mg/L initial concentrations were transferred into separate flasks. 0.15 g of selected CPUF (CAc-PPUF), was added into each flask. The pH of all test solutions were 6.5. Batch adsorption experiments were carried out as described in Section 2.2.3.

2.7. Determination of the Adsorption Isotherm Model

In this study, the isotherm models Langmuir, Freundlich, Sips and Dubinin-Astakhov were examined since they are most frequently utilized in the aqueous phase adsorption experiments. According to Tran et al.'s (2017), the parameters of the isotherm models were found by a nonlinear optimization technique using Microsoft Office Excel program (Microsoft Corp., USA). The obtained models were assessed using the normalized root mean square error (NRMSE), the correlation coefficient (R^2), and the Chi square (X^2).

3. RESULTS AND DISCUSSION

3.1. Comparison of adsorption capacities of different cellulose based adsorbents for Cu, Co and Ni ions

The target heavy metals experiments were carried out under different experimental conditions using six different cellulose based adsorbents. Batch adsorption experiments were performed by adding a constant dose of cellulose based adsorbent into 100 mg/L aqueous Cu^{2+}, Co^{2+} and Ni^{2+} solutions. The adsorption capacity and heavy metal removal efficiency of each cellulose based adsorbent for Cu, Co, and Ni ions were determined under the given conditions. The results are presented in Figure 3.1.

Cu ion adsorption capacities of the PUF samples tested, AC-HMPUF, AC-PPUF, CAc-PPUF, CAc-HMPUF, CMC-PPUF and CMC-HMPUF, were 1.04 mg/g, 1.15 mg/g, 5.59 mg/g, 1.44 mg/g, 3.18 mg/g and 3.54 mg/g, respectively. PUF samples displayed 0 mg/g, 1.53 mg/g, 2.82 mg/g, 1.22 mg/g, 1.07 mg/g, and 2.59 mg/g Ni ion adsorption capacities, respectively. Surface concentrations of Co ion were 3.84 mg/g for CAc-PPUF, and 1.51 mg/g for CMC-HMPUF while no detectable adsorption capacity was obtained for the other PUF samples tested.

Cu ion removal rates of AC-HMPUF, AC-PPUF, CAc-PPUF, CAc-HMPUF, CMC-PPUF, and CMC-HMPUF were 10.21%, 11.26%, 62.42%, 14.12%, 31.24% and 35%, while the Ni ion removal rates were 0%, 12.56%, 23.2%, 10.02%, 8.76%, and 21.31%, respectively. Co ion was removed at 36.39% efficiency by CAc-PPUF, and 14.35% efficiency by CMC-HMPUF.

These results show that CAc-PPUF has a higher removal efficiency for the metal ions Cu^{2+}, Co^{2+}, and Ni^{2+} compared to the other PUF samples tested with the observed removal efficiencies of 62.42%, 36.39%, and 23.2%, respectively. In general, inter-molecular interactions between surface functional groups of carbon-based adsorbents, and heavy metals are rather complex, and depend on the heterogeneity and chemistry of the adsorbent surface, ionic conditions of the aqueous solution, and the chemistry of adsorbate. Heavy metals may bind to carbon-based adsorbents via physical adsorption, electrostatic interaction, ion exchange, surface complexation, and precipitation. Depending on the target metal ion, ionic environment of the solution, and the carbon-based adsorbent, the precise function of each process in heavy metal adsorption varies

greatly (Yang et al., 2019). Harvey et al. 2011, reported that hard Lewis base functional groups, such as deprotonated carboxylic acids and phenols, enhance sorption while soft Lewis base functional groups, such as carbonyl and aromatic structures, encourage dipole-dipole interactions, such as cation-bonding for Cd^{+2} adsorption (Harvey et al., 2011). Zhang et al., (2022), evaluated the adsorption properties of different functional groups containing N or O atoms. They showed that adsorbents containing negatively charged -COO- or $–SO_3$- groups presented excellent adsorption capacities for cationic heavy metals (Zhang et al., 2022). Therefore, the substantially higher removal efficiencies attained by CAc-PPUF may be due to the presence of -COO- functional groups contained by the cellulose acetate based polyurethane foam adsorbent.

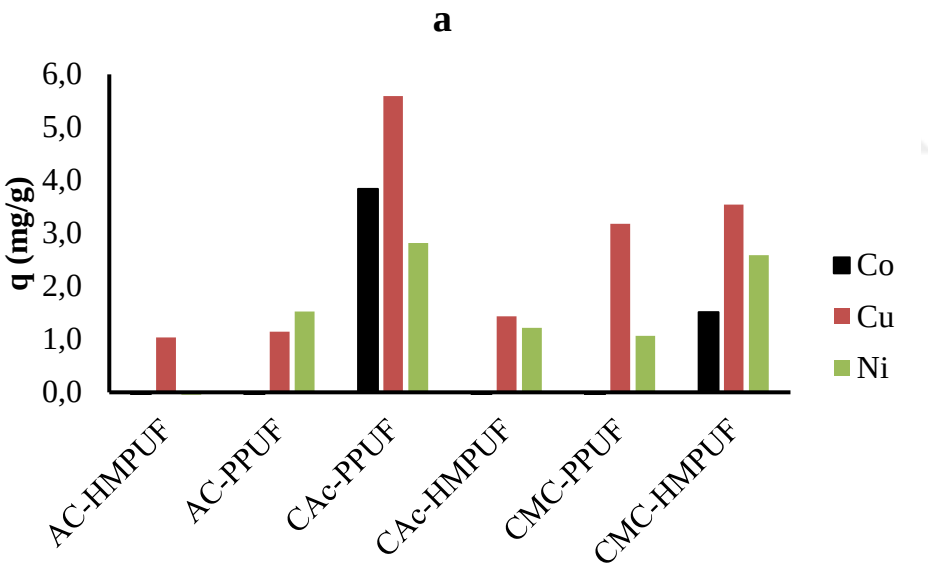

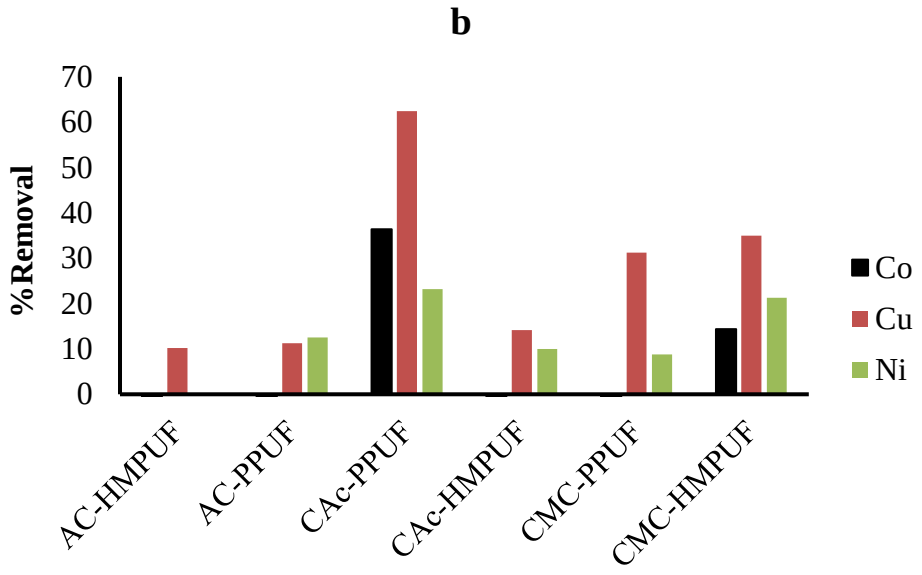

Figure 3.1. a) Comparison of adsorption capacity and b) %removal efficiencies for Cu, Co and Ni ions on different adsorbents (pH= 6.5, Initial heavy metal concentration= 100 ppm, t =24°C, time=24 hours)

3.2. Material Characterization

3.2.1. FTIR Results

In order to verify the functional groups contained in the CAc-PPUF, Fourier transform infrared spectroscopy (FTIR) method was used. The respective FTIR curve in transmission mode is presented in Figure 3.2. The peaks at 3300 cm^{-1} for N-H, and at 1656 cm^{-1} for CO-NH are the evidence for urethane linkage by the condensation reaction between OH groups of cellulose acetate, and CNO groups of 1,4-phenylene diisocyanate. The symmetric and asymmetric stretching vibration absorbance bands for C-H of the aromatic ring are detected at 2933, and 2910 cm^{-1}, respectively. The strong absorbance band at 1740 cm^{-1} indicates the presence of carbonyl, C=O, functional group of cellulose acetate. The wide band from 3672 to 2940 cm^{-1} is due to the stretching vibrations of hydroxyl groups. The intensities of the absorption bands at 1627, and 1507 cm^{-1} are due to C=C stretching in the aromatic ring. The sharp peaks detected at 1215, and 1034 cm^{-1} display the presence of C–O–C stretch vibrations. As a result, the FTIR spectrum of CAc-PPUF confirms its proposed structure shown in Figure 3.2.

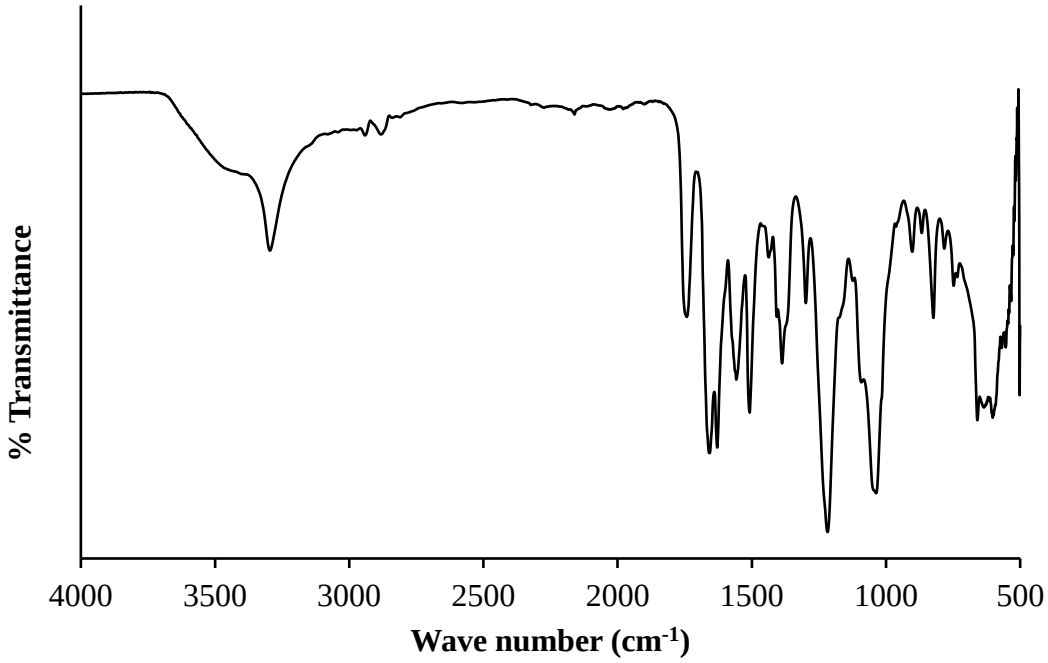

Figure 3.2. FTIR result for CAc-PPUF

3.2.2. SEM Results

The surface examination of CAc-PPUF was carried out using QUANTA 400F Field Emission SEM with high resolution. Additionally, energy dispersive X-ray spectroscopy (EDAX) was adapted for the elemental analysis of synthesized CAc-PPUF. Typical SEM images obtained for CAc-PPUF between the scale range of 2 - 20 μm can be seen in Figure 3.3 SEM images exhibit a highly porous amorphous structure with variable micropore spaces.

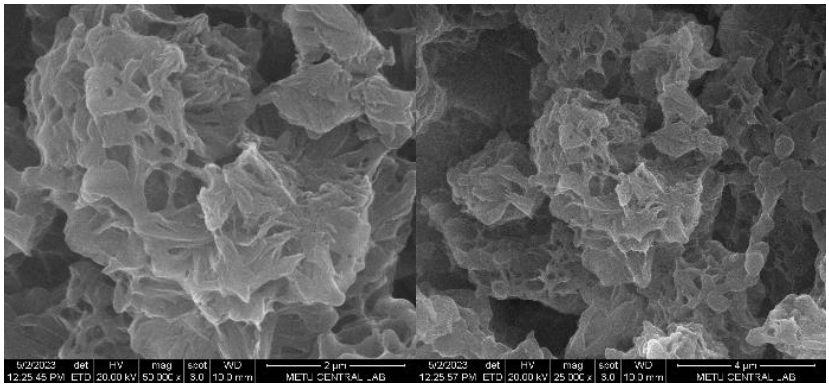

a) 2 μm b) 4 μm

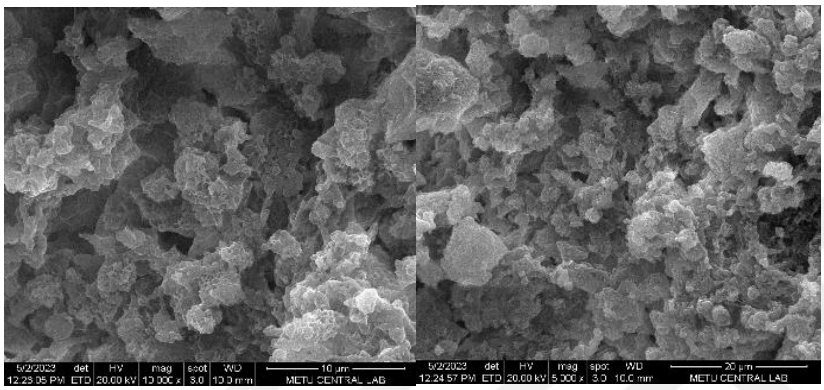

c) 10 μm d) 20 μm

Figure 3.3. SEM images of CAc-PPUF a) 2 μm b) 4 μm c) 10 μm d) 20 μm

EDAX results identified 78.31% carbon, and 21.69 % oxygen in the structure. EDAX results were not able to identify the nitrogen atoms in the structure. This may be due to the fact that there are relatively few nitrogen atoms in CAc-PPUF compared to carbon and oxygen atoms.

3.2.3. BET Results

Surface area, and pore size distribution (PSD) are important characteristics of adsorbent materials because they have significant impact on the adsorption performance (Mukhtar et al., 2020b). One of the most common techniques used to determine the surface area of adsorbents is the Brunauer-Emmett-Teller (BET) technique. A continuous flow of an inert gas, such as nitrogen, is applied to the adsorbent sample during the BET procedure. Nitrogen gas molecules adsorb to the surface, and the pores of the adsorbent due to the weak van der Waals forces, and form an adsorbed gas monolayer. The specific surface area (m^2/g), and the pore structure of the adsorbent can be estimated using the nitrogen

gas adsorption-desorption isotherms (George & Stephen Brunauer, 1938). In this study, CAc-PPUF was subjected to nitrogen sorption hysteresis at 77.40 K using Quantachrome Corporation, Autosorb-6. The N_2 adsorption–desorption isotherms, and the corresponding PSD curve for CAc-PPUF are shown in Figs. 3.4 (a) and (b), respectively.

As can be seen in Figure 3.4 a, according to the IUPAC classification, the resultant isotherm can be categorized as type-IV with an H3 hysteresis loop. Type-IV N_2 adsorption-desorption isotherm signifies mesoporous solids. The large H3 hysteresis loop formed by the adsorption and desorption branches of the isotherm is due to capillary condensation taking place in mesopores by increasing relative pressure. It further confirms the mesoporous nature of CAc-PPUF (Thommes et al., 2015). Additionally, H3 hysteresis indicates pores with a slit form (Mohammadi et al., 2011). The pore size distribution curve of CAc-PPUF is shown in Figure 3.4 b. The Barrett-Joyner-Halenda (BJH) model estimates the average pore radius of CAc-PPUF to be 19.96 nm, further supporting the mesoporous (2–50 nm in size) nature of CAc-PPUF (Thommes et al., 2015). The BET surface area of CAc-PPUF, calculated from the quantity of monolayer of nitrogen gas adsorbed, is 23.15 m^2/g.

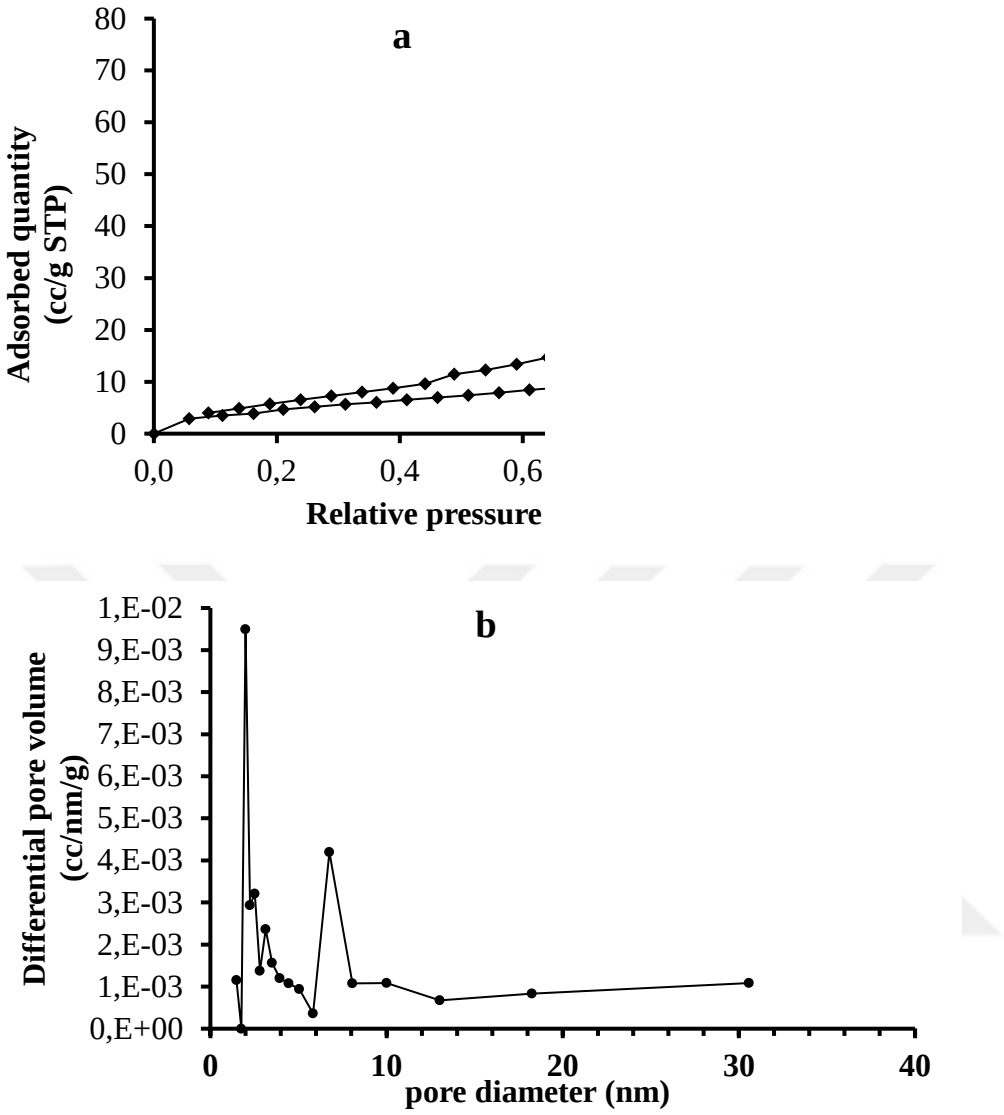

Figure 3.4. (a) N2 Adsorption-Desorption Isotherm of CAc-PPUF, (b) Pore size distribution curve of CAc-PPUF

3.2.4. Zeta potential

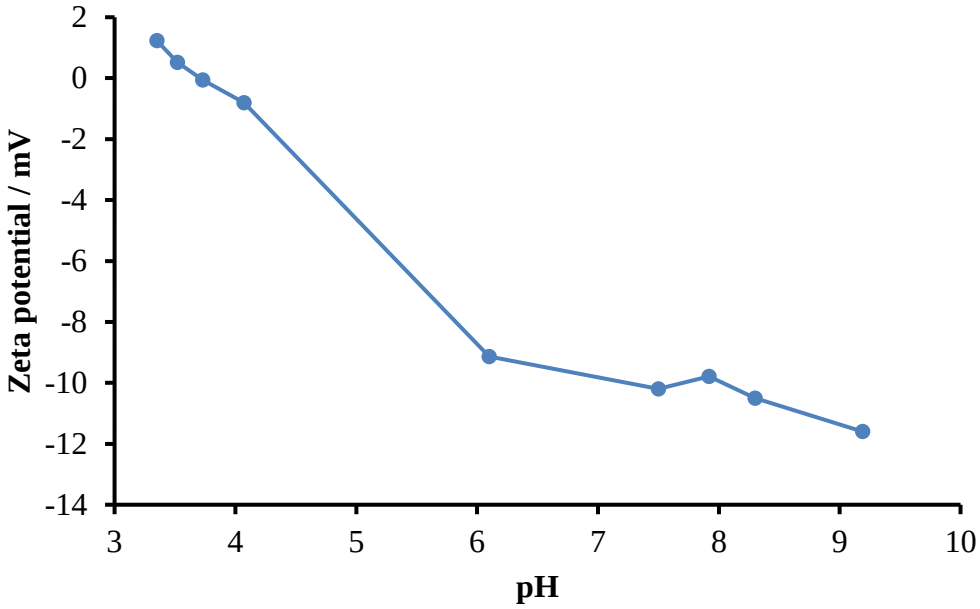

Figure 3.5. The effect of pH on zeta potential

Zeta potential versus pH graph of CAc-PPUF is shown in Figure 3.5. Figure 3.5 illustrates a gradual reduction in zeta potential of CAc-PPUF as pH increases (H^+ ion concentration decreases). Zeta potential is 1.23 at pH 3.35. It reaches to 0 at around pH 3.73. At pH 9 it decreases to -12 mV. When the pH is 4 or higher, zeta potential of CAc-PPUF is negative. This shows that the surface of CAc-PPUF, in the pH range of 4 to 9 is negatively charged, which makes it a promising foam material for the removal of heavy metals since heavy metal ions are positively charged in water.

Elimelech, 1994 reported that the Zeta potential of cellulose acetate at all pH values was negative. The zeta potential of the cellulose acetate was evaluated over the pH range of 3-11, and it was negative at all pH values mentioned. The pH values greater than 4.5, the Zeta potential becomes increasingly negative as ionic strength increases (Elimelech et al., 1994).

3.3. Adsorption isotherm models

Monolayer adsorption onto the homogeneous surface is described by the Langmuir isotherm model (Langmuir, 1918). This model's basic assumptions are uniform energy adsorption, reversible adsorption, and the absence of interaction between adsorption

species on a surface with a finite number of accessible sites.

It is presumable that once the adsorbent site is completely covered by the adsorbent no more adsorption takes place there. Additionally, it implies that all adsorption sites have an identical energy level (Jasper et al., 2020).

The nonlinear form of Langmuir isotherm model is written as follows:

$$q_e = \frac{Q^o_{max} K_L C_e}{1 + K_L C_e} \quad (3.1)$$

where, Q_{max} is the maximum monolayer adsorption capacity evaluated from Langmuir model(mg /g); K_L is Langmuir constant (L /mg), Ce is the equilibrium concentration of the solute(mg/L).

The most popular model, the Langmuir isotherm, is based on the idea that monolayer coverage only occurs at specific homogeneous sites with a constant number of identical and energetically equivalent adsorption sites and no deviation into the plane of the adsorbent surface (Dubey et al., 2016).

The Freundlich isotherm model is idely utilized in heterogeneous surfaces with non-uniform energy distribution of active sites and interaction between adsorbent molecules (Freundlich, 1907). It can be used to adsorb over multiple layers.

Unlike the Langmuir isotherm model, the Freundlich model is not restricted to monolayer adsorption and can also be applied to multilayer adsorption (Chen et al., 2022).

The nonlinear form of Freundlich isotherm model is written as follows:

$$q_e = K_F C_e^{1/n} \quad (3.2)$$

where K_F is the Freundlich constant associated with adsorption capacity and 1/n is the heterogeneity factor. A large value of the adsorption capacity K_F, indicates a higher adsorption capacity.

Sips isotherm is a hybrid model that results from the combination of both Langmuir and Freundlich isotherm models. Adsorbent surfaces can either be homogeneous or heterogeneous (Sips, 1948).

The Sips model is the best of the three parametric isotherms for predicting monolayer

adsorption in homogenous and heterogeneous systems as it avoids the limitations of increased concentrations of the adsorbate associated with the Freundlich model (Chen et al., 2022).

The non-linear form of Sip isotherm equation is written as follows:

$$q_e = \frac{q_m^S K_S C_e^{1/n_S}}{1 + K_S C_e^{1/n_S}} \quad (3.3)$$

where, q_m^S (mg/g) is the maximum sips adsorption capacity; Ks (L /mg) is the Sips isotherm constant; n_S is the Sips isotherm model exponent also known as heterogeneity factor. Homogeneous adsorption occurs when n_s is one, whereas heterogeneous adsorption occurs when n_s is less than one (Chen et al., 2022).

Models based on the Dubinin-Astakhov (D-A) isotherm were frequently employed for adsorption research in aqueous solutions. In order to understand how gases and vapors adhere to microporous adsorbents, the D-A model was initially devised by (Dubinin and Astakhov in 1971).

3.4. Evaluation of isotherm models for heavy metal adsorption on CAc-PPUF

During the isotherm studies, the initial concentrations of Cu^{2+}, Co^{2+}, and Ni^{2+} in the test solutions were varied between 20-100 mg/L by keeping the CAc-PPUF adsorbent dose constant. The equilibrium sorption data obtained for the three heavy metals were tested for two parameter isotherms (Langmuir and Freundlich) and three parameter isotherms (Sips and Dubinin-Astakhov) using the non-linear regression method. These models are well known isotherm models in aqueous phase adsorption studies. Such models help to get information related to surface characteristics, adsorbate adsorbent affinity, adsorption capacity, and favorability of the sorption process.

3.4.1. Cobalt ion adsorption isotherm models on CAc-PPUF

As described in Chapter 2, non-linear regression method was used, to predict the model parameters, and to determine the goodness of fit measures. Experimental data, which involve equilibrium heavy metal concentrations remaining in solution, C_e, and the corresponding q_e values, and the initial estimates of the unknown model parameters were entered into the Excel Spreadsheet. Theoretical q_e values were calculated for a range of C_e values between 0-60 mg/L. Initial estimates were changed by several iterations until

the lowest possible value of NRMSE between the experimental data and the theoretical model output was obtained. Thus, the model parameters were selected. Then, the goodness of fit measures were calculated. The model parameters for the four selected isotherm models, and the goodness of fit measures for Co ion adsorption by CAc-PPUF are presented in Table 3.1. Figure 3.6 presents the experimental data and the isotherm model predictions for Co ion. As can be seen in Table 3.1, and Figure 3.6, the four selected isotherm model predictions are highly comparable. R^2, χ^2, and NRMSE values range between 0.918-0.936, 0.076-0.132, and 0.089-0.101, respectively. Dubinin-Astakhov (DA) model, however, has a relatively higher R^2 (0.936), lower χ^2 (0.094), and NRMSE 0.089. DA model can be applied to describe the adsorption of solutes on structurally heterogeneous adsorbents (Gil and Grange, 1996). Heterogeneous adsorbents carry different types of binding sites with various binding energies. One frequently anticipated aspect of engineered materials, such as functionalized carbons as synthesized in this study, is the binding site heterogeneity (Kumar et al., 2019). CAc-PPUF has several binding sites such as acetate groups, oxygen, and nitrogen atoms to interact with heavy metal ions. Therefore, the DA adsorption isotherm model is selected to describe the Co ion adsorption onto CAc-PPUF. Table 3.4 shows a Comparison of Co ion adsorption onto CAc-PPUF with different adsorbents evaluated in the literature

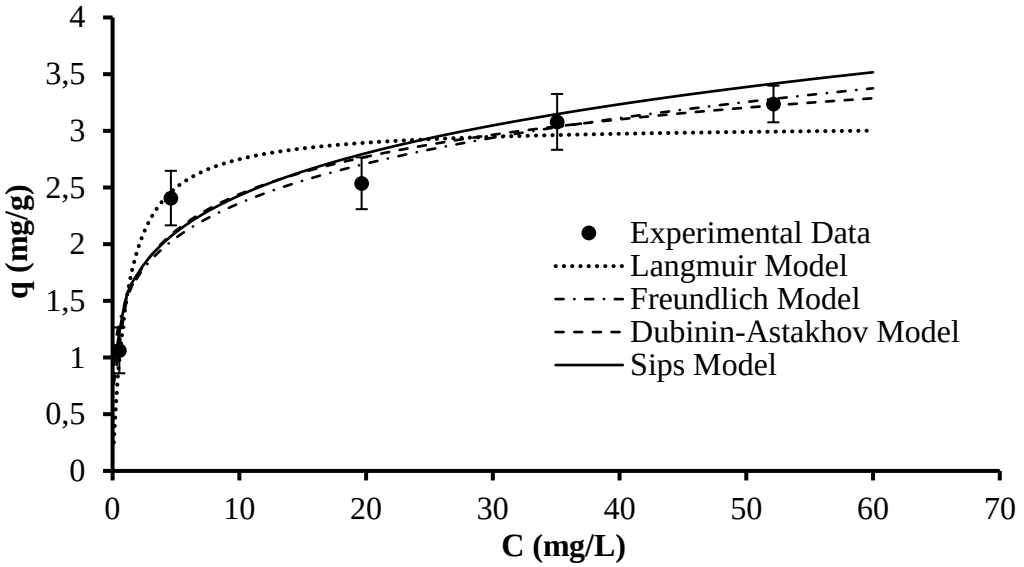

Figure 3.6. Testing isotherm models for Co^{2+} adsorption by CAc-PPUF (pH= 6.5, t =24°C, time=24 hours)

Table 3.1. Isotherm model parameters, and goodness of fit measures for Co ion on CAc-PPUF

Model	Equation	Model Parameters	Goodness of fit measures
Langmuir	$q_e = \frac{Q^o_{max} K_L C_e}{1 + K_L C_e}$	Q_{max} (mg/g) = 3.1 K_L (L/mg) = 0.893	R^2 = 0.929 χ^2 = 0.076 NRMSE = 0.094
Freundlich	$q_e = K_F C_e^n$	K_F ((mg/g)/(mg/L)^n)=1.491 n = 0.1994	R^2 = 0.918 χ^2 = 0.132 NRMSE = 0.101
Sips	$q_e = \frac{q^S_m K_S C_e^{1/n_S}}{1 + K_S C_e^{1/n_S}}$	q^S_m (mg/g) = 84.5 K_S (mg/L)$^{-1/nS}$ = 0.018 $1/n_S$ = 0.207	R^2 = 0.919 χ^2 =0.130 NRMSE = 0.101
Dubinin-Astakhov	$q_e = q_{DA\,(max)} \cdot \exp\left\{-K_{DA}\left[RT \ln\left(\frac{C_S}{C_e}\right)\right]^{n_{DA}}\right\}$	$q_{DA\,(max)}$ (mg/g) = 3.953 K_{DA} ((mol/kJ)^{nDA})=0.0004 n_{DA} = 1.569	R^2 = 0.936 χ^2 = 0.094 NRMSE = 0.089

where q_e (mg/g) is the amount of Co^{2+} uptake at equilibrium; Ce (mg/L) is the equilibrium concentration of Co; Qmax (mg/g) is the maximum adsorption capacity calculated from Langmuir model; K_L (L/mg) is Langmuir constant; K_F ((mg/g)/(mg/L)n) is the Freundlich constant; n (dimensionless) is the Freundlich intensity parameter; q_{ms} (mg/g) is the maximum adsorption capacity calculated from Sip model; Ks is Sips equilibrium constant (mg/L) -1/nS, 1/nS is the Sips heterogeneity constant; $q_{DA(max)}$ (mg/g) is the maximum adsorption capacity estimated from Dubinin-Astakhov model; K_{DA} (mol/J)n_{DA} a constant related to sorption energy; C_s (mg/L) is the aqueous solubility of Co^{2+} at the given temperature; n_{DA} is the heterogeneity factor of Dubinin-Astakhov isotherm.

3.4.2. Copper ion adsorption isotherm models on CAc-PPUF

By entering the remaining Cu^{+2} concentrations in solution, and the corresponding qe values, into the excel spreadsheet, which generates the theoretical q_e values according to the four selected isotherm models, model parameters, and the goodness of fit measures were obtained as shown in Table 3.2. Theoretical qe values were obtained for the C_e range of 0 and 60 mg/L. The experimental results and the predictions for Cu ion using the isotherm model equations are shown in Figure 3.7.

Three out of four chosen isotherm model predictions are very comparable. R^2 and $\chi 2$ values and NRMSE values range from 0.919-0.991, 0.044-2.131, and 0.035-0.105. As shown in Table 3.2, according to the statistical analysis, Freundlich, Sips, and Dubinin-Astakhov models are best fit models for the Cu^{2+} adsorption isotherm with high R^2 and low $\chi 2$ and NRMSE values. As mentioned earlier, these models describe the adsorption process onto a heterogeneous surface. Since the surface of CAc-PPUF is heterogeneous, these models are effectively predicting the observed results. According to Vijayaraghavan et al., 2006, there is no critical reason to use complex models if two parameter models can fit the kinetics data well. Therefore, we can select the Freundlich isotherm model as the best –fit model (Jasper et al., 2020). Table 3.6 shows a Comparison of Cu ion adsorption onto CAc-PPUF with different adsorbents evaluated in the literature.

Table 3.2. Isotherm models and goodness of fit measures of Cu ion on CAc-PPUF

Model	**Model Parameters**	**Goodness of fit measures**
Langmuir	Q_{max} (mg/g) = 6.4 K_L (L/mg) = 0.139	R^2 = 0.919 χ^2 = 2.131 NRMSE = 0.105
Freundlich	K_F ((mg/g)/(mg/L)^n) = 1.557 n = 0.3409	R^2 = 0.991 χ^2 = 0.049 NRMSE = 0.035
Sips	q_m^S (mg/g) = 93.5 K_S (mg/L)$^{-1/nS}$ = 0.017 $1/n_S$ = 0.356	R^2 = 0.9906 χ^2 = 0.054 NRMSE = 0.036

Dubinin-Astakhov	$q_{DA\ (max)}$ (mg/g) = 14.040 K_{DA} ((mol/kJ)^{nDA}) = 0.0202 n_{DA} = 0.935	R^2 = 0.991 χ^2 =0.044 NRMSE = 0.035

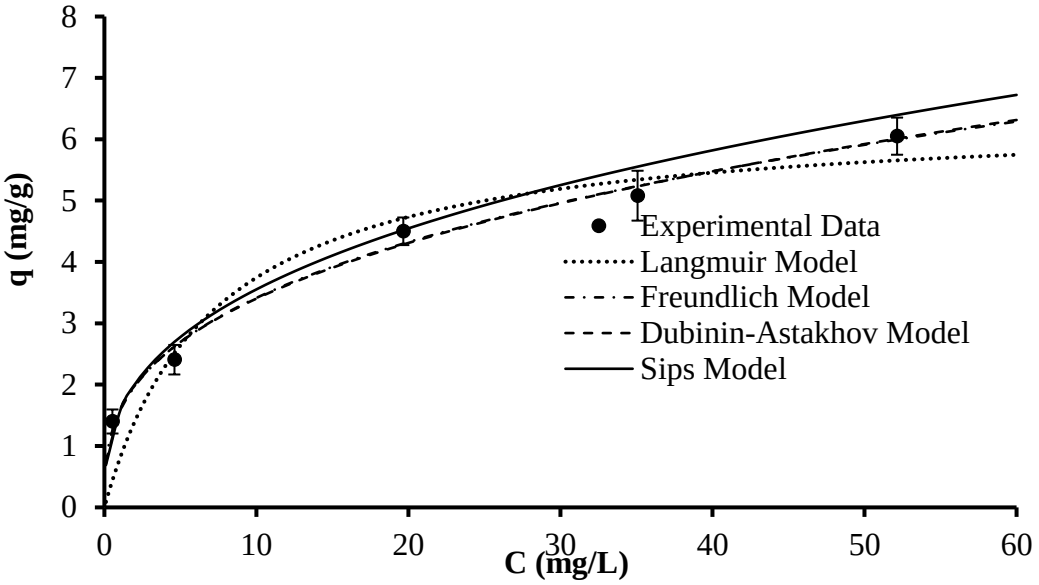

Figure 3.7. Testing isotherm models for Cu^{2+} adsorption by CAc-PPUF (pH= 6.5, t=24°C, time=24 hours)

3.4.3. Nickel ion adsorption isotherm models

Determination of the best-fit isotherm model for the sorption of Ni ions onto CAc-PPUF was evaluated using the method described above. Model predictions were determined for equilibrium Ni ion concentrations ranging between 0 to 85 mg/L, and theoretical qe values were estimated using Eqs (3.1), (3.2) and (3.3). Model parameters, and the goodness of fit measures for the tested model equations are shown in Table 3.3. The experimental results, and the model predictions for Ni ion adsorption are shown in Figure 3.8. As can be seen in Table 3.3, the predictions of the four tested isotherm models are quite similar. R^2, $\chi 2$ and NRMSE values range between 0.946-0.9965, 0.006-0.120, and 0.021-0.084, respectively. However, three parameter isotherm models (Sips and Dubinin-Astakhov) were observed to show slightly better fits to the experimental data of the Ni^{2+} isotherm on CAc-PPUF. The results displayed the highest performance

with high R^2 values (0.9961, 0.9965, respectively), whereas $\chi 2$ (0.006-0.008, respectively), and NRMSE (0.022-0.021, respectively) values of Sips and Dubinin-Astakhov were close to zero, as shown in Table 3.3.

Yousef et al (2016) studied the adsorption isotherms for the removal of Ni^{2+} by an ion-exchange resin from aqueous solutions were examined. They also reported that three parameter isotherm models such as Dubinin-Astakhov and Sips could be used to describe the adsorption isotherm with high accuracy. Table 3.5 shows a Comparison of Ni ion adsorption onto CAc-PPUF with different adsorbents evaluated in the literature.

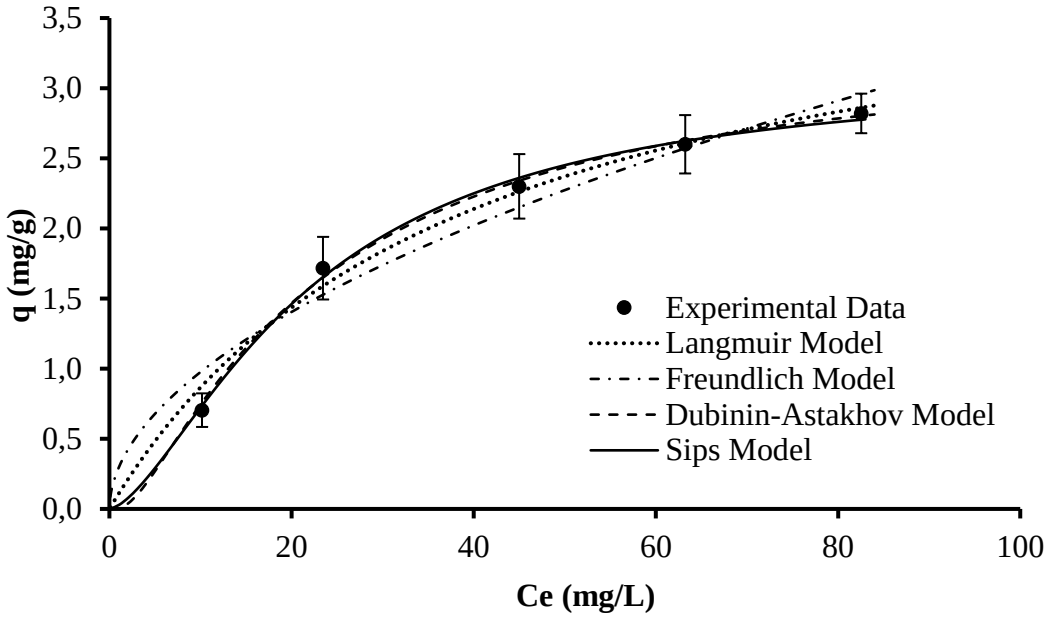

Figure 3.8. Testing isotherm models for Ni^{2+} adsorption by CAc-PPUF (pH= 6.5, t=24℃, time=24 hours)

Table 3.3. Isotherm models and goodness of fit measures of Ni ion on CAc-PPUF

Model	**Model Parameters**	**Goodness of fit measures**
Langmuir	Q_{max} (mg/g) = 4.2 K_L (L/mg) = 0.026	R^2 = 0.983 χ^2 = 0.046 NRMSE = 0.047
Freundlich	K_F ((mg/g)/(mg/L)^n) = 0.291 n = 0.5255	R^2 = 0.946 χ^2 = 0.120 NRMSE = 0.084
Sips	q_m^S (mg/g) = 3.1 K_S (mg/L)$^{-1/nS}$ = 0.008 $1/n_S$ = 1.548	R^2 = 0.9961 χ^2 = 0.006 NRMSE = 0.022
Dubinin-Astakhov	$q_{DA\ (max)}$ (mg/g) = 3.139 K_{DA} ((mol/kJ)^{nDA}) = 0.000 n_{DA} = 3.276	R^2 = 0.9965 χ^2 =0.008 NRMSE = 0.021

Table 3.4. Comparison of Co ion adsorption onto CAc-PPUF with different adsorbents evaluated in the literature

Adsorbent	Contact time (h)	Concentration Rate (mg/L)	Adsorbent dose (g/L)	Adsorption capacity (mg/g)	pH	Reference
Al-pillared bentonite clay	24	10-25	2	38.6	6	(Manohar et al., 2006)
Hydroxyapatite	24	5-1000	-	20.19	-	(Smičiklas et al., 2006)
Kaolinite	2	0-2400	1	0.919	-	(Yavuz et al., 2003)
Lemon peel as biosorbent	10	0-1000	10	22	6	(Bhatnagar et al., 2010)
Coir pith	2	20-50	2	12.82	4.3	(Parab et al., 2006)
Natural zeolites	5.5	100-400	20	14.38	6-7	(Erdem et al., 2004)
Almond green hull	0.12	-	0.25	45.5	-	(Ahmadpour et al., 2009)
Unmodified silica gel	50	80	2	2	5	(Repo et al., 2009)
CAc-PPUF	24	100	10	3.84	6.5	Present study

Table 3.5. Comparison of Ni ion adsorption onto CAc-PPUF with different adsorbents evaluated in the literature

Adsorbent	Contact time (h)	Concentration Rate (mg/L)	Adsorbent dose (g/L)	Adsorption capacity (mg/g)	pH	Reference
Kaolinite	2	300	2	2.3	-	(Yavuz et al., 2003)
Coir pith	2	50	2	15.3	6	(Parab et al., 2006)
Modified silica gel	50	80	2	14.1	4	(Repo et al., 2009)
Peat	4	100	5	14	5-7	(Bartczak et al., 2018)
Waste pea shell	0.67	100	5	25.77	-	(Kamil Öden et

						al., 2022)
Natural clay	2	100	5	1.138	6	(Es-Sahbany et al., 2019)
CAc-PPUF	24	100	10	2.82	6.5	Present study

Table 3.6. Comparison of Cu ion adsorption onto CAc-PPUF with different adsorbents evaluated in the literature

Adsorbent	Contact time (h)	Concentration Rate (mg/L)	Adsorbent dose (g/L)	Adsorption capacity (mg/g)	Reference
Kaolinite	2	300	1	9.5	(Yavuz et al., 2003)
Shells of lentil	3	100	2	3.92	(Aydin et al., 2008)
Shells of wheat	3	100	1	2.71	(Aydin et al., 2008)
Shells of rice	3	100	2	1.09	(Aydin et al., 2008)
Natural biomass Alga sargassum muticum	4	15-190	5	71	(Carro et al., 2015)
Saccharomyces cerevisiae biomass	-	25-200	15	2.59	(Renu et al., 2017)
Cellulose acetate	0.25	1	0.035	0.93	(Kamaruzaman et al., 2017).
CAc-PPUF	24	100	10	5.59	Present study

3.5. Adsorption kinetics

Adsorption kinetics describes the rate at which a given adsorbent removes a specific adsorbate. When planning and modeling adsorption systems, kinetic parameters offer useful information on adsorption uptake processes (Dubey et al., 2016). Therefore, in this study, adsorption kinetic models have been utilized to further assess the adsorption performance, and the adsorption mass transfer mechanisms of heavy metals by CAc-PPUF. Cu^{2+} was selected as the representative heavy metal ion. In this regard, several 100 ppm solutions of Cu^{2+} were subjected to CAc-PPUF adsorption for different time intervals. At the end of the pre-defined period of time, CAc-PPUF was separated from the test solutions by filtration, and the residual Cu^{2+} concentration was assessed using AAS. Compatibility of the experimental data with three well-known kinetic models; pseudo-first order (PFO), pseudo-second order (PFO), and Elovich, was evaluated using the non-linear regression method described earlier.

The empirical pseudo first order form of kinetic equation is written as follows: (Vareda, 2023)

$$q_t = qe\,(1 - e^{-K_1 t}) \qquad (3.4)$$

where qe and qt are the amount of adsorbate adsorbed (mg/g) at equilibrium and at time t (min), respectively, and k_1 (min^{-1}) is the pseudo-first-order rate constant.

The empirical pseudo second order form of kinetic equation is written as follows: (Jasper et al., 2020).

$$Qt = \frac{qe^2 k2t}{1+qek2t} \qquad (3.5)$$

where qe and qt are the amounts of heavy metal adsorbed (mg/g) at equilibrium and at time t (min), respectively, and k_2 (g/ mg min) is the pseudo-second-order rate constant.

The Elovich equation was first developed to describe the kinetics of chemisorption of gas onto solids. The non-linear form of the Elovich equation is presented by the following equation: (Yousef et al., 2016).

$$qt = \frac{1}{\beta}\ \ln(1 + \alpha\beta t) \qquad (3.6)$$

where β is extent of surface coverage and activation energy, and α is the initial sorption

rate constant (mg/g min).

Figure 3.9 shows change in Cu ion concentration with respect to time by CAc-PPUF. From Figure 3.9, it is observed that the adsorption process reaches equilibrium in 70 minutes. Based on the results of the experiments, the kinetic models were evaluated.

The model parameters for the three selected isotherm models, and the goodness of fit measures for Cu ion adsorption by CAc-PPUF are presented in Table 3.5. Figure 3.9 shows the experimental data and of kinetics model predictions for the Cu ion. As can be seen in Table 3.5, and Figure 3.9, the three selected kinetic model predictions are highly comparable. R^2, χ^2, and NRMSE values range between 0.974-0.991, 0.064-0.171, and 0.030-0.052, respectively. In this study, kinetic data for Cu^{2+} adsorption on CAc-PPUF were described by pseudo-second order (PSO) model. PSO, however, displayed a comparatively greater R^2 (0.991), lower χ^2 (0.064), and NRMSE (0.03). Therefore, the pseudo-second order (PSO) model with a PSO rate constant of 0.009281 g/(mg x min) best describes the kinetics of copper ion adsorption onto CAc-PPUF surface under the given experimental conditions.

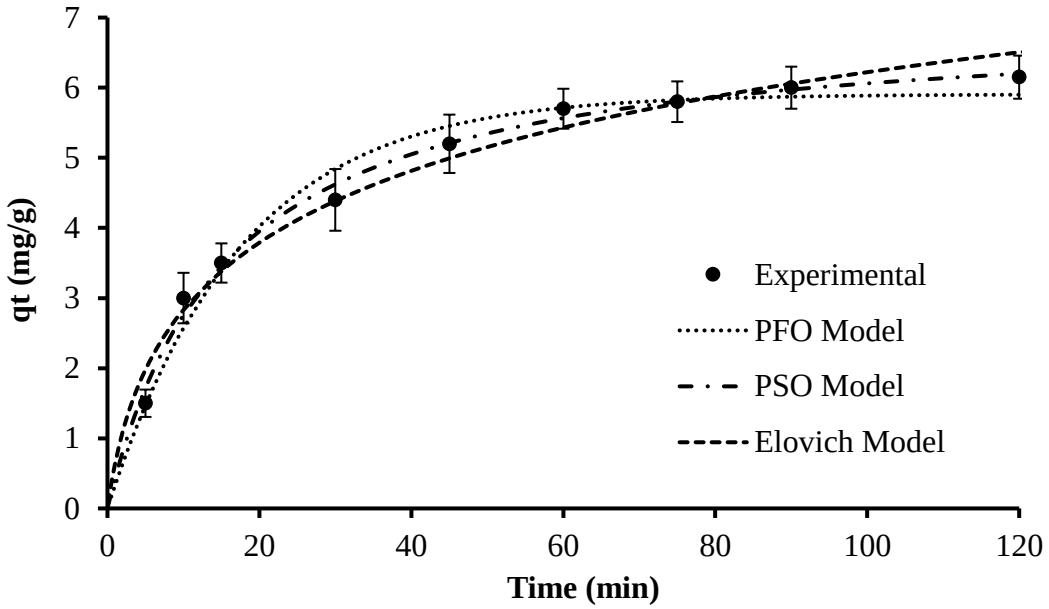

Figure 3.9. Kinetic data for Cu^{2+} adsorption on CAc-PPUF (pH= 6.5, t=25°C, initial concentration=100 ppm, time=24 hours)

Table 3.7. kinetic models for Cu ion adsorption on CAc-PPUF

Model	Model constants	R^2	χ^2	NRMSE
PFO	K_1 = 0.057 min^{-1}	0.974	0.142	0.052
PSO	K_2 = 0.009281 g/(mg x min)	0.991	0.064	0.030
Elovich	α = 0.786 mg/(g*min) β = 0.630826 g/mg	0.975	0.171	0.051

Keys: k_1 g/ (mg x min) is the pseudo-first-order rate constant; k_2 g/ (mg x min) is the pseudo-second-order rate constant; α is the initial sorption rate constant (mg/g min); β is extent of surface coverage and activation energy; qe (mg/g) and qt are the amounts of heavy metal adsorbed at equilibrium and at time t (min), respectively.

3.6. Effect of pH

The electrostatic interaction between the heavy metal ion, and the surface groups of adsorbent strongly depends on solution pH since the surface charges of carbon-based materials vary depending on the pH. The ionization of surface groups has a significant impact on the charged interface between carbons and the solution. When the concentration of H^+ ions that protonate the surface functional groups falls below Ka of the surface groups, the surfaces of carbon-based adsorbents become positively charged (Duan et al., 2020).

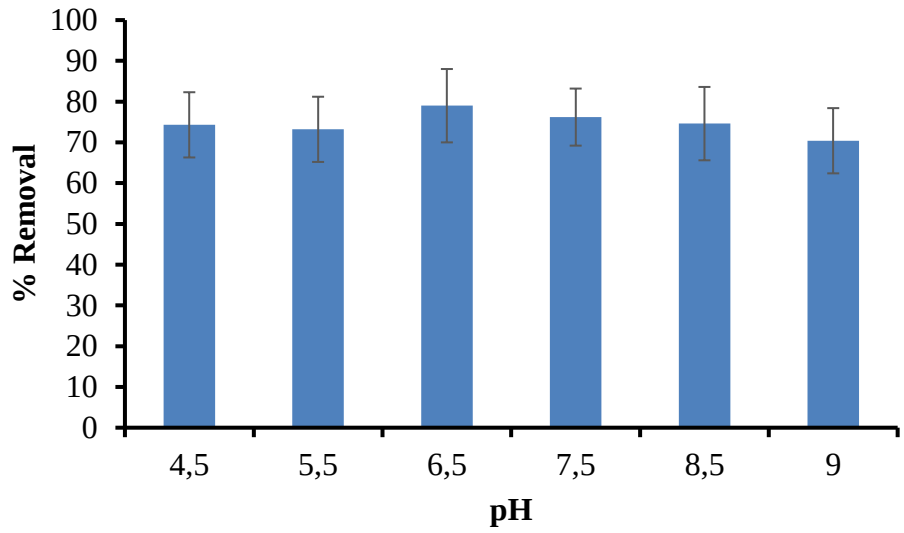

Figure 3.10. Change in %removal capacity with respect to the pH (t=25°C, initial Cu concentration=60 ppm, time=24 hours)

Figure 3.10 indicates that there is no statistically significant difference in %removal capacity with respect to pH where the pH ranges from 4.5 to 9 and the initial concentration was 60 ppm of Cu ion solution. As Figure 3.10 reflects, the surface charge of CAc-PPUF is negative at or above pH 4. Therefore, varying solution pH between 4.5 and 9 does not have a significant effect on Cu ion removal under the given conditions.

3.7. Effect of temperature

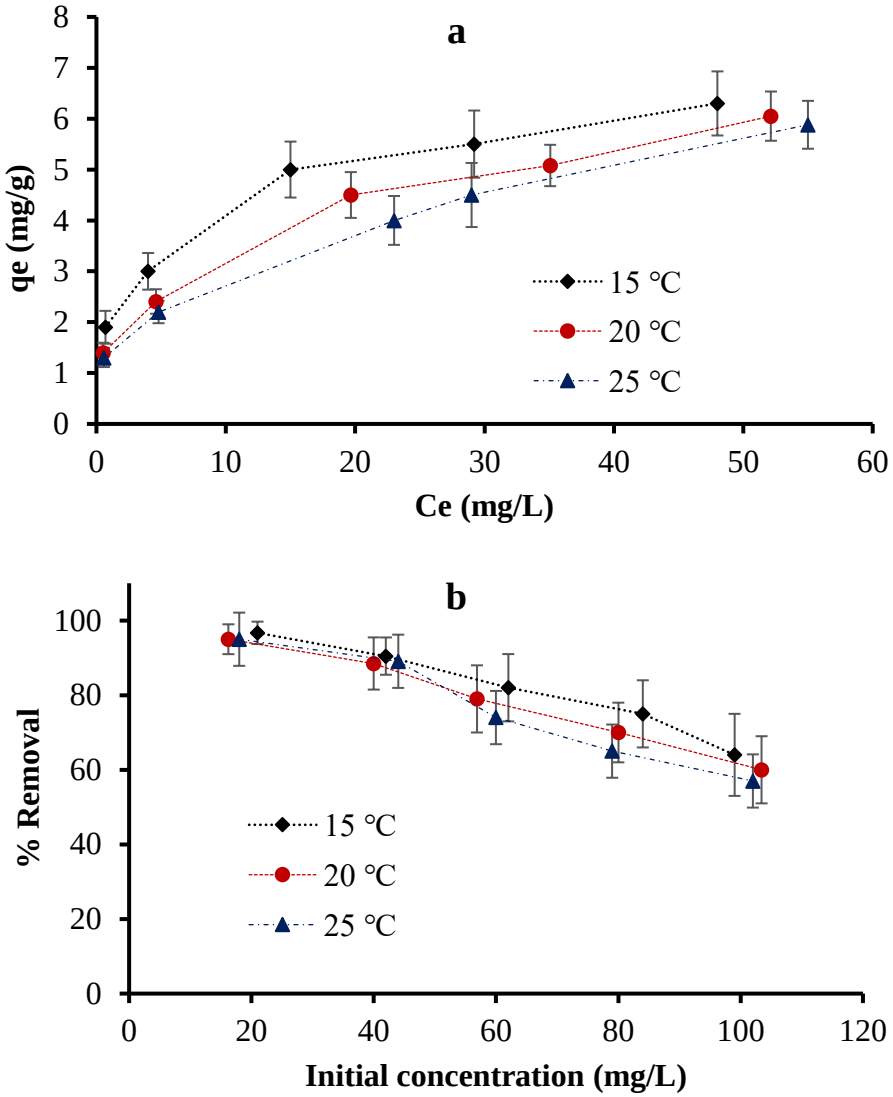

Figure 3.11. a) Changing adsorption capacity with respect to temperature. b) Change in %removal capacity with respect to temperature (pH= 6.5, time=24 hours).

In Figure 3.11, data show that there is no significant temperature effect. However, the adsorption capacity at 15℃ is slightly higher than 25℃, which suggests an exothermic adsorption reaction.

3.8. Reuse study

Reusability of the newly synthesized CAc-PPUF was assessed by conducting five Cu^{2+} adsorption-desorption cycles. As described earlier, after each cycle, the used CAc-PPUF samples were treated with 1 M HCl solution to promote the desorption of Cu^{2+}. % Cu ion removal efficiencies determined during each cycle are presented in Figure 3.12. Figure 3.12 shows that the %removal was slightly reduced from 79% to 67.4% during five cycles. The efficacy of Cu ion elimination is almost maintained up to five cycles. This observation reveals that the adsorbed Cu ions can be efficiently recovered by treating CAc-PPUF with 1M HCl solution for one hour. Furthermore, CAc-PPUF can be reused up to five cycles without a significant reduction in the removal efficiency.

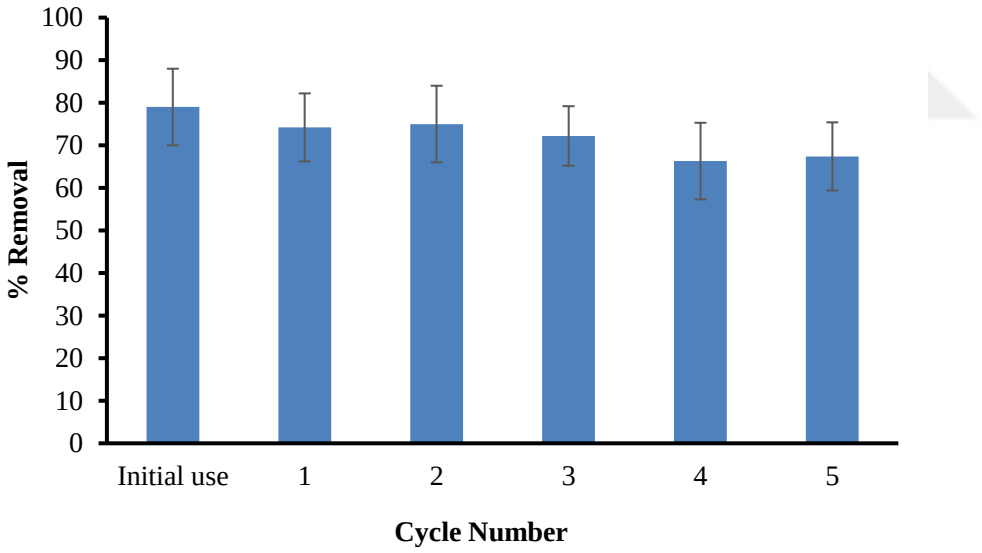

Figure 3.12. % Cu ion removal efficiency of each adsorption-desorption cycle (pH= 6.5, t=25℃, initial Cu concentration=60 ppm, time=24 hours)

3.9. Real water Sample Treatment

Table 3.8. Metal contamination of groundwater sample from Palestine

Metal ions	Concentration in groundwater sample (ppm)	Metal ions	Concentration in groundwater sample (ppm)	Metal ion	Concentration In groundwater sample (ppm)
Be	0.008	**Na**	2309	**Bi**	0.224
Ca	1530	**Zn**	8.819	**Co**	0.029
Cr	0.372	**V**	1.211	**Cu**	1.564
Fe	69.821	**U**	0.025	**Rb**	0.284
Ga	0.031	**Sr**	5.401	**Ni**	14.202
K	211.035	**Li**	0.143	**Pb**	0.159

A groundwater sample from Palestine was analyzed by ICP-MS for its metal ion content, and Table 3.6 displays the concentrations that were obtained. The applicability of CAc-PPUF for the removal of Co, Cu, Ni, Cr, Pb and Zn ions from the water sample was tested by adding CAc-PPUF into several 50 mL water samples at 0.1 g/L concentrations. The samples were shaken for 2 hours at 25 ℃, and then the samples were filtered with 0.2 μm PTFE filter. The remaining heavy metal concentrations after adsorption were measured by ICP-MS, and the removal efficiencies were calculated. Treatment with

CAc-PPUF removed more than 90% of Co, Cu, Cr, Pb, and Zn ions. Ni ion removal, however, was lower, almost 51 %. It can be due to the relatively higher Ni ion concentration, and competition due to the presence of other metal ions. Except Ni ions, other metals were comparable to Turkish Drinking Water Standard after treatment with CAc-PPUF. This result shows that CAc-PPUF can be effectively used as an adsorbent for the removal of heavy metal ions from contaminated groundwaters.

4. Conclusions

The purpose of this work was to develop cellulose-based adsorbent foam materials that are inexpensive and include ionic functional groups that can remove heavy metals efficiently. In this regard, six different cellulose based foam adsorbents (AC-HMPUF, AC-PPUF, CAc-PPUF, CAc-HMPUF, CMC-PPUF and CMC-HMPUF) were synthesized. Heavy metal removal capacity of each synthesized foam sample was tested for the removal of Co^{2+}, Cu^{2+}, and Ni^{2+} ions as the model heavy metals.

The removal of Co^{2+}, Cu^{2+}, and Ni^{2+} ions by the cellulose based foam adsorbents synthesized at the outset of the study was assessed under identical conditions. The results made it possible to identify the best adsorbent structure for heavy metal removal. At 100 mg/L initial heavy metal concentration, 10 g/L adsorbent dose, and pH of 6.5, CAc-PPUF revealed a superior efficiency for the removal of Co, Ni and Cu ions from aqueous solutions with 62.42%, 36.39% and 23.2% removal efficiencies, respectively. The greatest adsorption capacity was determined by CAc-PPUF to be 5.59 mg/g for the Cu ion. Therefore, CAc-PPUF was employed as the adsorbent material in all of the batch adsorption experiments in the subsequent sections of the study.

CAc-PPUF was characterized by Fourier Transform Infrared Analysis (FTIR), Scanning Electron Microscopy (SEM), Brunauer-Emmett-Teller (BET), and Zeta Potential analyses. The proposed structure of CAc-PPUF was confirmed by FTIR analysis. SEM exhibits a highly porous amorphous structure with variable micropore spaces. The mesoporous nature of CAc-PPUF was studied using BET analysis which reveals that the average pore radius of the material is 19.96 nm while the surface area is 23.15 m^2/g. The zeta potential of CAc-PPUF at pH 3.35 is 1.23. It reaches to zero at a pH of about 3.73. It drops to -12 mV at pH 9. In the pH range of 4 to 9, the zeta potential of CAc-PPUF demonstrated a negatively charge. This is attributed to the low Ka values of surface functional groups. Negative zeta potential of CAc-PPUF over a wide pH range makes it a promising adsorbent for the removal of heavy metals since heavy metal ions are positively charged in water.

Batch adsorption experiments were conducted to examine the Cu^{2+}, Co^{2+} and Ni^{2+} isotherm models from aqueous solution under different experimental conditions such as pH, initial metal ion concentration, heavy metal dosage, contact time and temperature

were investigated. CAc-PPUF was revealed an excellent efficiency for the removal of Co, Ni and Cu ions from aqueous solutions with the corresponding findings are 62.42%, 36.39% and 23.2%. The highest adsorption capacity of Cu ion by CAc-PPUF was attained at 5.59 mg/g.

Adsorption isotherms for heavy metal removal onto CAc-PPUF were investigated by varying the initial heavy metal ion concentrations in solution between 20-100 mg/L. It was observed that the effectiveness of CAc-PPUF at removing heavy metals from aqueous solutions was inversely proportional to the initial concentration of heavy metals in solution. For example, it was found that when the initial copper ion concentration was increased to 100 mg/L, the removal efficiency fell to 60.0% from 98.7% at the initial copper ion concentration of 20 mg/L. Similarly, the removal efficiency was found to be 96.7% at a starting cobalt ion concentration of 20 mg/L, but it fell to 49.6% at an initial concentration of 100 mg/L. For all the initial concentrations tested, it was found that nickel ion removal efficiencies were inferior to those determined for copper and cobalt ions. Nickel ion removal efficiency was 65.0% at an initial concentration of 20 mg/L, and decreased to 17.5% at an initial concentration of 100 mg/L.

The equilibrium sorption data obtained for the three heavy metals were tested for two parameter isotherms (Langmuir and Freundlich) and three parameter isotherms (Sips and Dubinin-Astakhov) using the non-linear regression method. When the fit of the four tested isotherm models to the experimental data are evaluated statistically, it is observed that the models result in highly comparable predictions. Freundlich, Sips, and Dubinin-Astakhov models have slightly better fits for Cu^{2+} adsorption. DA model had statistically better predictions for cobalt ion adsorption onto CAc-PPUF. Three parameter isotherm models (Sips and Dubinin-Astakhov) were observed to show slightly better fits to the experimental data for the Ni^{2+} isotherm on CAc-PPUF. These models are applied to describe the adsorption of solutes on structurally heterogeneous adsorbents. CAc-PPUF has several binding sites such as acetate groups, oxygen, and nitrogen atoms to interact with heavy metal ions. Therefore, these findings are in good agreement with the heterogeneous functional groups of CAc-PPUF.

The adsorption kinetics of Cu ion on CAc-PPUF was investigated at 100 mg/L initial Cu ion concentration, 10 g/L adsorbent dose, and pH of 6.5. The results were analyzed

based on pseudo-first order (PFO), pseudo-second order (PSO) and Elovich models. Pseudo-second order (PSO) model revealed a superior efficiency with a relatively higher R^2 (0.991), and lower χ^2 (0.064) and NRMSE (0.03). The pseudo-second order reaction rate constant was 0.009281 g/ (mg x min) and the equilibrium time was 120 min.

Varying solution pH between 4.5 and 9 does not have a significant effect on Cu ion removal when the initial concentration is 60 ppm of Cu ion. It was also shown that there is no significant temperature effect. However, the adsorption capacity at 15℃ is slightly higher than 25℃, which suggests an exothermic adsorption reaction.

The desorption and reuse studies of CAc-PPUF were investigated using 1M HCl solution. The adsorption capacity was not changed significantly in the reusability study when five adsorption-desorption experiments were conducted. The %removal was slightly reduced from 79% to 67.4% during five cycles.

In the final stage of the study, the applicability of CAc-PPUF for the removal of Co, Cr, Cu, Pb and Zn ions were tested using real environmental water samples from groundwater. Other than Ni ion, all the other heavy metal ions were removed more 90%. Ni ion, however, was removed almost 51 %. This suggests that CAc-PPUF can be effectively used as adsorbent for the removal of heavy metal ions in water and wastewater treatment.

The aim of this study was to assess the efficiency of cellulose based foam for the removal of heavy metal ions from aqueous solutions. It was confirmed that CAc-PPUF can be used as a novel foam material for the removal of heavy metals.

REFERENCES

Ahmadpour, A., Tahmasbi, M., Bastami, T.R., Besharati, J.A., 2009. Rapid removal of cobalt ion from aqueous solutions by almond green hull. J Hazard Mater 166, 925–930.

Aşçi, Y., Kaya, Ş., 2014. Removal of cobalt ions from water by ion-exchange method. Desalination Water Treat 52, 267–273.

Aydin, H., Bulut, Y., Yerlikaya, Ç., 2008. Removal of copper (II) from aqueous solution by adsorption onto low-cost adsorbents. J Environ Manage 87, 37–45.

Azra, N., Nazir, F., Roosh, M., Khalid, M.A., Mansoor, M.A., Bahadar Khan, S., Iqbal, M., 2022. Extraction of Pb (II) and Co (II) using N,N-dioctylsuccinamate based room temperature ionic liquids containing aliphatic and aromatic cations. Arabian Journal of Chemistry 15.

Bartczak, P., Norman, M., Klapiszewski, Ł., Karwańska, N., Kawalec, M., Baczyńska, M., Wysokowski, M., Zdarta, J., Ciesielczyk, F., Jesionowski, T., 2018. Removal of nickel(II) and lead(II) ions from aqueous solution using peat as a low-cost adsorbent: A kinetic and equilibrium study. Arabian Journal of Chemistry 11, 1209–1222.

Bhatnagar, A., Minocha, A.K., Sillanpää, M., 2010. Adsorptive removal of cobalt from aqueous solution by utilizing lemon peel as biosorbent. Biochem Eng J 48, 181–186.

Carriço, C.S., Fraga, T., Pasa, V.M.D., 2016. Production and characterization of polyurethane foams from a simple mixture of castor oil, crude glycerol and untreated lignin as bio-based polyols. Eur Polym J 85, 53–61.

Chen, X., Hossain, M.F., Duan, C., Lu, J., Tsang, Y.F., Islam, M.S., Zhou, Y., 2022. Isotherm models for adsorption of heavy metals from water - A review. Chemosphere.

Chfadi, T., Gheblawi, M., Thaha, R., 2021. Public acceptance of wastewater reuse: New evidence from factor and regression analyses. Water (Switzerland) 13.

Costa, J.M., Costa, J.G. dos R. da, Almeida Neto, A.F. de, 2022. Techniques of nickel(II) removal from electroplating industry wastewater: Overview and trends. Journal of Water Process Engineering.

Ding, W., Liang, H., Zhang, H., Sun, H., Geng, Z., Xu, C., 2023. A cellulose/bentonite grafted polyacrylic acid hydrogel for highly-efficient removal of Cd(II). Journal of Water Process Engineering 51.

Duan, C., Ma, T., Wang, J., Zhou, Y., 2020. Removal of heavy metals from aqueous solution using carbon-based adsorbents: A review. Journal of Water Process Engineering.

Dubey, S., Gusain, D., Sharma, Y.C., 2016. Kinetic and isotherm parameter determination for the removal of chromium from aqueous solutions by nanoalumina, a nanoadsorbent. J Mol Liq 219, 1–8.

Dutta, A.S., 2018. Polyurethane Foam Chemistry, in: Recycling of Polyurethane Foams. Elsevier, pp. 17–27.

Dyer, C.A., 2005. 5 Heavy Metals as Endocrine-Disrupting Chemicals.

Elimelech, M., Chen, W.H., Waypa, J.J., 1994. Measuring the zeta (electrokinetic) potential of reverse osmosis membranes by a streaming potential analyzer.

Erdem, E., Karapinar, N., Donat, R., 2004. The removal of heavy metal cations by natural zeolites. J Colloid Interface Sci 280, 309–314.

Es-Sahbany, H., Berradi, M., Nkhili, S., Hsissou, R., Allaoui, M., Loutfi, M., Bassir, D., Belfaquir, M., Youbi, M.S. El, 2019. ScienceDirect Removal of heavy metals (nickel) contained in wastewater-models by the adsorption technique on natural clay.

Ezeonuegbu, B.A., Machido, D.A., Whong, C.M.Z., Japhet, W.S., Alexiou, A., Elazab, S.T., Qusty, N., Yaro, C.A., Batiha, G.E.S., 2021. Agricultural waste of sugarcane bagasse as efficient adsorbent for lead and nickel removal from untreated wastewater: Biosorption, equilibrium isotherms, kinetics and desorption studies. Biotechnology Reports 30.

Furtwengler, P., Perrin, R., Redl, A., Avérous, L., 2017. Synthesis and characterization of polyurethane foams derived of fully renewable polyester polyols from sorbitol. Eur Polym J 97, 319–327.

Gautam, G.J., Chaube, R., 2018. Differential effects of heavy metals (Cadmium, cobalt, lead and mercury) on oocyte maturation and ovulation of the Catfish Heteropneustes

fossilis: An In Vitro study. Turk J Fish Aquat Sci 18, 1205–1214.

George, A., Stephen Brunauer, B., n.d. 03s Adsorptıon Of Gases In Multımolecular Layers 300 Contrıbutıon From The Bureau Of Chemıstry And Sons Adsorption of Gases in Multimolecular Layers.

Georgescu, B., Georgescu, C., Dărăban, S., Bouaru, A., Paşcalău, S., 2011. Heavy Metals Acting as Endocrine Disrupters, Scientific Papers: Animal Science and Biotechnologies.

Gianì, F., Masto, R., Trovato, M.A., Malandrino, P., Russo, M., Pellegriti, G., Vigneri, P., Vigneri, R., 2021. Heavy metals in the environment and thyroid cancer. Cancers (Basel).

Gil, A., Grange, P., 1996. COLLOIDS A Application of the Dubinin-Radushkevich and Dubinin-Astakhov equations in the characterization of microporous solids, Colloids and Surfaces SURFACES A: Physicochemical and Engineering Aspects.

Harvey, O.R., Herbert, B.E., Rhue, R.D., Kuo, L.J., 2011. Metal interactions at the biochar-water interface: Energetics and structure-sorption relationships elucidated by flow adsorption microcalorimetry. Environ Sci Technol 45, 5550–5556.

Heinze, T., El Seoud, O.A., Koschella, A., 2018. Cellulose Activation and Dissolution. pp. 173–257.

Heinze, T., Liebert, T., Klüfers, P., Meister, F., 1999. Carboxymethylation of cellulose in unconventional media *, Cellulose.

Jasper, E.E., Ajibola, V.O., Onwuka, J.C., 2020. Nonlinear regression analysis of the sorption of crystal violet and methylene blue from aqueous solutions onto an agro-waste derived activated carbon. Appl Water Sci 10.

Jia, X., Zhang, L., Zhao, J., Ren, M., Li, Zewu, Wang, J., Wang, S., Liu, Y., An, H., Li, Y., Yan, L., Li, Zhiwen, Liu, X., Pan, B., Ye, R., 2021. Associations between endocrine-disrupting heavy metals in maternal hair and gestational diabetes mellitus: A nested case-control study in China. Environ Int 157.

Kamaruzaman, S., Fikrah Aris, N.I., Yahaya, N., Hong, L.S., Raznisyafiq Razak, M., 2017. Removal of Cu (II) and Cd (II) Ions from Environmental Water Samples by Using

Cellulose Acetate Membrane. Journal of Environmental Analytical Chemistry 04.

Kamil Öden, M., Karasakal, E.N., Çildir, S., 2022. Nickel (II) Removal from Synthetic Wastewater by Adsorption Using Waste Pea Shell. International Journal of Environmental Trends (IJENT) 6, 10–20.

Kausar, A., Zohra, S.T., Ijaz, S., Iqbal, M., Iqbal, J., Bibi, I., Nouren, S., El Messaoudi, N., Nazir, A., 2023. Cellulose-based materials and their adsorptive removal efficiency for dyes: A review. Int J Biol Macromol.

Kubra, K.T., Salman, M.S., Hasan, M.N., Islam, A., Hasan, M.M., Awual, M.R., 2021. Utilizing an alternative composite material for effective copper(II) ion capturing from wastewater. J Mol Liq 336.

Kumar, V., Parihar, R.D., Sharma, A., Bakshi, P., Singh Sidhu, G.P., Bali, A.S., Karaouzas, I., Bhardwaj, R., Thukral, A.K., Gyasi-Agyei, Y., Rodrigo-Comino, J., 2019. Global evaluation of heavy metal content in surface water bodies: A meta-analysis using heavy metal pollution indices and multivariate statistical analyses. Chemosphere.

Liu, M., Deng, Y., Zhan, H., Zhang, X., 2002. Adsorption and desorption of copper(II) from solutions on new spherical cellulose adsorbent. J Appl Polym Sci 84, 478–485.

Liu, Y., Fan, H., Wang, X., Zhang, J., Li, W., Wang, R., 2022. Controllable synthesis of bifunctional corn stalk cellulose as a novel adsorbent for efficient removal of Cu2+ and Pb2+ from wastewater. Carbohydr Polym 276.

López-Botella, A., Velasco, I., Acién, M., Sáez-Espinosa, P., Todolí-Torró, J.L., Sánchez-Romero, R., Gómez-Torres, M.J., 2021. Impact of heavy metals on human male fertility—An overview. Antioxidants.

Manohar, D.M., Noeline, B.F., Anirudhan, T.S., 2006. Adsorption performance of Al-pillared bentonite clay for the removal of cobalt(II) from aqueous phase. Appl Clay Sci 31, 194–206.

Mohammadi, M., Najafpour, G.D., Mohamed, A.R., 2011. Dobijanje ugljeničnih molekulskih sita iz palmine ljuske depozicijom ugljenika iz metana. Chemical Industry and Chemical Engineering Quarterly 17, 525–533.

Mukhtar, A., Mellon, N., Saqib, S., Lee, S.P., Bustam, M.A., 2020a. Extension of BET theory to CO2 adsorption isotherms for ultra-microporosity of covalent organic polymers. SN Appl Sci 2.

Oyewo, O.A., Elemike, E.E., Onwudiwe, D.C., Onyango, M.S., 2020. Metal oxide-cellulose nanocomposites for the removal of toxic metals and dyes from wastewater. Int J Biol Macromol.

Parab, H., Joshi, S., Shenoy, N., Lali, A., Sarma, U.S., Sudersanan, M., 2006. Determination of kinetic and equilibrium parameters of the batch adsorption of Co(II), Cr(III) and Ni(II) onto coir pith. Process Biochemistry 41, 609–615.

Pinto, M.L., 2010. Formulation, preparation, and characterization of polyurethane foams. J Chem Educ 87, 212–215.

Qu, J., Tian, X., Jiang, Z., Cao, B., Akindolie, M.S., Hu, Q., Feng, C., Feng, Y., Meng, X., Zhang, Y., 2020. Multi-component adsorption of Pb(II), Cd(II) and Ni(II) onto microwave-functionalized cellulose: Kinetics, isotherms, thermodynamics, mechanisms and application for electroplating wastewater purification. J Hazard Mater 387.

Rengaraj, S., Moon, S.-H., 2002. Kinetics of adsorption of Co(II) removal from water and wastewater by ion exchange resins, Water Research.

Renu, Agarwal, M., Singh, K., 2017. Heavy metal removal from wastewater using various adsorbents: A review. Journal of Water Reuse and Desalination.

Repo, E., Kurniawan, T.A., Warchol, J.K., Sillanpää, M.E.T., 2009. Removal of Co(II) and Ni(II) ions from contaminated water using silica gel functionalized with EDTA and/or DTPA as chelating agents. J Hazard Mater 171, 1071–1080.

Sayyed, A.J., Pinjari, D. V., Sonawane, S.H., Bhanvase, B.A., Sheikh, J., Sillanpää, M., 2021. Cellulose-based nanomaterials for water and wastewater treatments: A review. J Environ Chem Eng.

Sinha, S., Nigam, S., Solanki, S., Batra, L., Chug, P., Singh, R., 2023. Prospects on arsenic remediation using organic cellulose-based adsorbents. Ind Crops Prod 201, 116928.

Sips, R., 1948. On the structure of a catalyst surface. J Chem Phys 16, 490–495.

Smičiklas, I., Dimović, S., Plećaš, I., Mitrić, M., 2006. Removal of Co2+ from aqueous solutions by hydroxyapatite. Water Res 40, 2267–2274.

Srivastava, V., Sarkar, A., Singh, S., Singh, P., de Araujo, A.S.F., Singh, R.P., 2017. Agroecological responses of heavy metal pollution with special emphasis on soil health and plant performances. Front Environ Sci.

Sun, Z., Yin, Y., An, Y., Deng, C., Wei, Z., Jiang, Z., Duan, X., Xu, X., Chen, J., 2022. A novel modified carboxymethyl cellulose hydrogel adsorbent for efficient removal of poisonous metals from wastewater: Performance and mechanism. J Environ Chem Eng 10.

Thommes, M., Kaneko, K., Neimark, A. V., Olivier, J.P., Rodriguez-Reinoso, F., Rouquerol, J., Sing, K.S.W., 2015. Physisorption of gases, with special reference to the evaluation of surface area and pore size distribution (IUPAC Technical Report). Pure and Applied Chemistry 87, 1051–1069.

Vareda, J.P., 2023. On validity, physical meaning, mechanism insights and regression of adsorption kinetic models. J Mol Liq.

Vijayaraghavan, K., Padmesh, T.V.N., Palanivelu, K., Velan, M., 2006. Biosorption of nickel(II) ions onto Sargassum wightii: Application of two-parameter and three-parameter isotherm models. J Hazard Mater 133, 304–308.

Yang, X., Wan, Y., Zheng, Y., He, F., Yu, Z., Huang, J., Wang, H., Ok, Y.S., Jiang, Y., Gao, B., 2019. Surface functional groups of carbon-based adsorbents and their roles in the removal of heavy metals from aqueous solutions: A critical review. Chemical Engineering Journal.

Yavuz, O., -cin Altunkaynak, Y., uzel, F.G., 2003. Removal of copper, nickel, cobalt and manganese from aqueous solution by kaolinite, Water Research.

Yousef, N.S., Farouq, R., Hazzaa, R., 2016. Adsorption kinetics and isotherms for the removal of nickel ions from aqueous solutions by an ion-exchange resin: application of two and three parameter isotherm models. Desalination Water Treat 57, 21925–21938.

Yurdakal, S., Garlisi, C., Özcan, L., Bellardita, M., Palmisano, G., 2019. (Photo)catalyst

characterization techniques: Adsorption isotherms and BET, SEM, FTIR, UV-Vis, photoluminescence, and electrochemical characterizations, in: Heterogeneous Photocatalysis: Relationships with Heterogeneous Catalysis and Perspectives. Elsevier, pp. 87–152.

The Council of the European Union, 1998. The quality of water intended for human consumption. Official journal of the European communities.

Environmental Protection Agency, U., of Water, O., 2018. 2018 Edition of the Drinking Water Standards and Health Advisories Tables (EPA 822-F-18-001).

World Health Organization, Guidelines for drinking-water quality, 2022. Fourth edition incorporating the first and second addenda. ISBN 978-92-4-004505-4.

Gaballah, I., Goy, D., Allain, E., Kilbertus, G., Thauront, J., 1997. Recovery of Copper through Decontamination of Synthetic Solutions Using Modified Barks.

Hacıosmanoğlu, G.G., Genç, S., Can, Z.S., 2021. Efficient removal of methyl orange from aqueous solutions using ulexite. Environ Technol Innov 22.

Michałowicz, J., 2014. Bisphenol A - Sources, toxicity and biotransformation. Environ Toxicol Pharmacol.

Paschoalini, A.L., Savassi, L.A., Arantes, F.P., Rizzo, E., Bazzoli, N., 2019. Heavy metals accumulation and endocrine disruption in Prochilodus argenteus from a polluted neotropical river. Ecotoxicol Environ Saf 169, 539–550.

Rajendran, S., Priya, A.K., Senthil Kumar, P., Hoang, T.K.A., Sekar, K., Chong, K.Y., Khoo, K.S., Ng, H.S., Show, P.L., 2022. A critical and recent developments on adsorption technique for removal of heavy metals from wastewater-A review. Chemosphere 303.

Topare, N.S., Wadgaonkar, V.S., 2022. A review on application of low-cost adsorbents for heavy metals removal from wastewater. Mater Today Proc.

Turkish Standards, 2005. Water intended for human consumption. Turkish Standard Institute. TS 266.

Dubinin, M.M., Astakhov, V.A., 1971. Development of the concepts of the volume filling of micropores in the adsorption of gases and vapors by microporous adsorbent.

Russ. Chem. Bull. 20, 3-7.

Freundlich, H., 1907. Uber die adsorption in losungen. Zeitschrift fur Phys. Chemie 57, 385-470.

Langmuir, I., 1918. The adsorption of gases on plane surfaces of glass, mica and platinum. J. Am. Chem. Soc. 40, 1361-1403.

APPENDIX A. Calibration Curve of different Heavy Metal

A.1. Calibration Curve of Copper Ion

To prepare copper standard solution, different concentrations were prepared (1, 2, 3, 4, and 5 ppm). The calibration curve of Cu^{+2} was created by using the AAS instrument through measuring the different absorbance values for the prepared standard solutions. To determine unknown concentrations based on the directly proportional relationship between absorbance and concentration. R^2 of Copper (Cu^{2+}) was shown higher than the target as shown in Figure A.1.

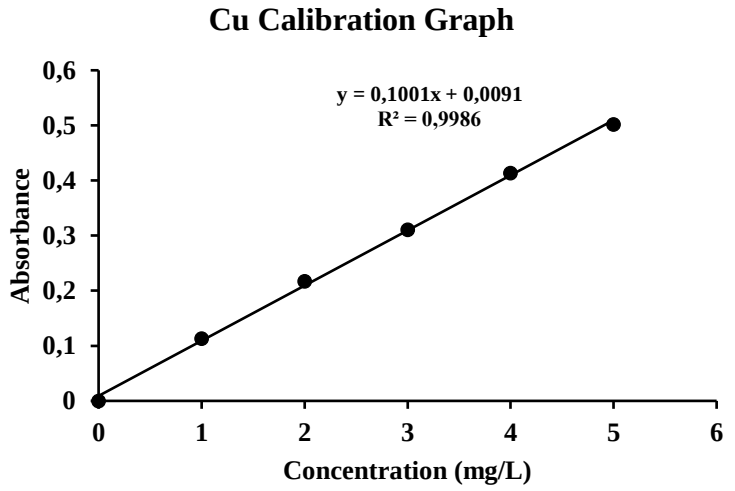

Figure A.1 Calibration curve of lead Cu^{2+}

A.2. Calibration Curve of Cobalt Ion

To prepare cobalt standard solution, different concentrations were prepared (0.5, 1, 1.5, 2, 3, and 4 ppm). The calibration curve of Co^{+2} was created by using the AAS instrument through measuring the different absorbance values for the prepared standard solutions. To determine unknown concentrations based on the directly proportional relationship between absorbance and concentration. R2 of Cobalt (Co^{2+}) was showed higher than the target as you can see in Figure A.2.

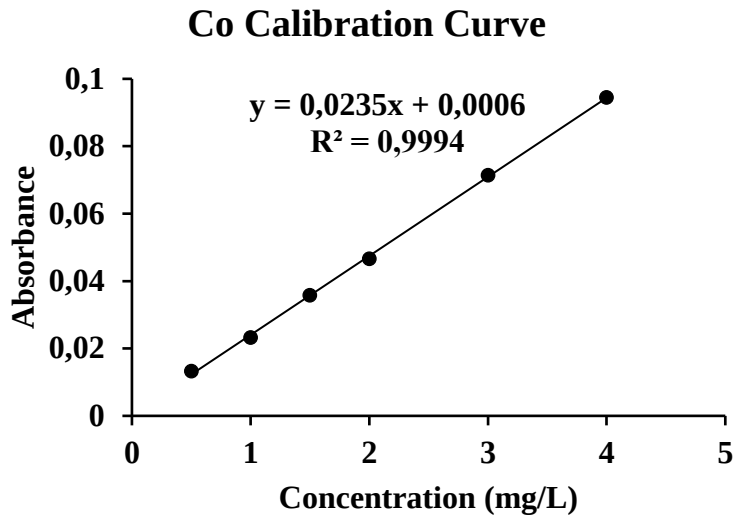

Figure A.2. Calibration curve of Cobalt Co^{2+}

A.3. Calibration Curve of Nickel Ion

To prepare nickel standard solution, different concentrations were prepared (0.5, 1, 1.5, 2, 3, and 4 ppm). The calibration curve of Ni^{+2} was created by using the AAS instrument through measuring the different absorbance values for the prepared standard solutions. To determine unknown concentrations based on the directly proportional relationship between absorbance and concentration. R^2 of nickel (Ni^{+2}) was shown higher than the target as you can see in Figure A.3.

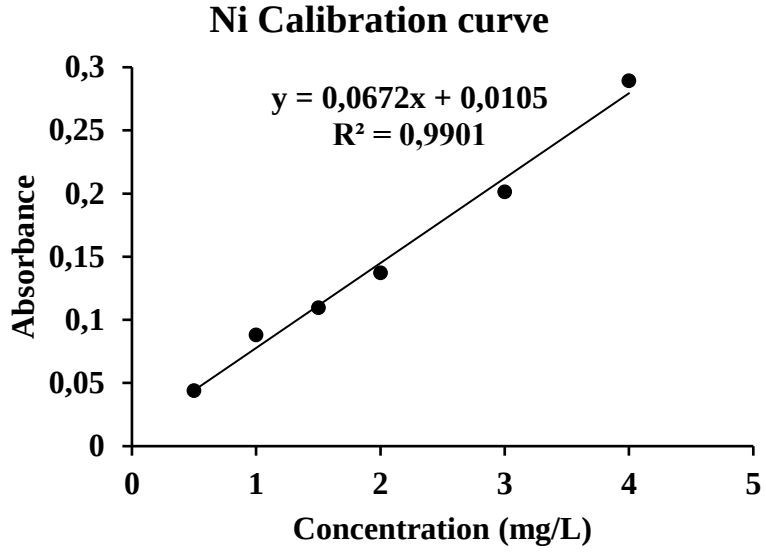

Figure A.3. Calibration curve of Nickel Ni^{2+}

CURRICULUM VITAE

LANGUAGES

Somali : Native

English : Excellent

Turkish : Excellent

Arabic : Good

EXPERIENCE

2022 – 2023 : Researcher

Marmara University, Environmental Engineering laboratory
Micropollutant removal from wastewater by using adsorption experiments and applicability of wastewater treatment plants.

2021 : Material Quality control

Horn of Africa Trading Company

2018 – 2019 : Site Engineer

Halgan Construction Company

2016 – 2017 : volunteer job

Wadajir General Trading & Contractors Co.

EDUCATION AND QUALIFICATIONS

Master : Environmental Engineering, Marmara University, 2023.
Bachelor : Civil Engineering, Mogadishu University, 2019.
Diploma : of Project Management, Mogadishu University, 2018.

SHORT COURSES ATTENDED

Courses	Status
Computer Application	Certificate
BOQ	Certificate
AutoCAD	Certificate
Arch CAD	Certificate
GIS	Certificate

REFERENCES

lecturer and researcher

Liban Mahi Moalim - Ministry of Petroleum& Mineral

Resource Director of Environment Department